

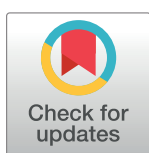
RESEARCH ARTICLE

Synthesis, molecular docking study and biological evaluation of new pyrrole scaffolds as potential antitubercular agents for dual targeting of enoyl ACP reductase and dihydrofolate reductase

Mater H. Mahnashi¹, Sravanthi Avunoori², Sanjay Gopi², Ibrahim Ahmed Shaikh³, Ahmed Saif⁴, Farkad Bantun⁵, Hani Saleh Faidah⁶, Abdulrahman Ali Alhadi⁶, Jaber Hassan Alshehri⁷, Abdullah Ali Alharbi⁷, Prem Kumar S. R.⁸, Shrinivas D. Joshi^{2*}

1 Department of Pharmaceutical Chemistry, College of Pharmacy, Najran University, Najran, Saudi Arabia, **2** Department of Pharmaceutical Chemistry, Novel Drug Design and Discovery Laboratory, SET's College of Pharmacy, Sangolli Rayanna Nagar, Dharwad, Karnataka, India, **3** Department of Pharmacology, College of Pharmacy, Najran University, Najran, Saudi Arabia, **4** Department of Clinical Laboratory Sciences, College of Applied Medical Sciences, King Khalid University, Abha, Saudi Arabia, **5** Faculty of Medicine, Department of Microbiology, Umm Al-Qura University, Makkah, Saudi Arabia, **6** Faculty of Medicine, Department of Microbiology, Umm Al-Qura University, Holy Makkah, Kingdom of Saudi Arabia, **7** Microbiology Section Pathology and Laboratory Medicine, Armed Forces Hospital Southern Region, Khamis Mushait, Kingdom of Saudi Arabia, **8** Department of Pharmaceutical Chemistry, MVM College of Pharmacy, Yelahanka, Bengaluru, Karnataka, India

* shrinivasdj@rediffmail.com



OPEN ACCESS

Citation: Mahnashi MH, Avunoori S, Gopi S, Shaikh IA, Saif A, Bantun F, et al. (2024) Synthesis, molecular docking study and biological evaluation of new pyrrole scaffolds as potential antitubercular agents for dual targeting of enoyl ACP reductase and dihydrofolate reductase. PLoS ONE 19(5): e0303173. <https://doi.org/10.1371/journal.pone.0303173>

Editor: Afzal Basha Shaik, Vignan Pharmacy College, INDIA

Received: December 12, 2023

Accepted: April 19, 2024

Published: May 13, 2024

Copyright: © 2024 Mahnashi et al. This is an open access article distributed under the terms of the [Creative Commons Attribution License](https://creativecommons.org/licenses/by/4.0/), which permits unrestricted use, distribution, and reproduction in any medium, provided the original author and source are credited.

Data Availability Statement: All relevant data are within the paper and its [Supporting Information](#) files.

Funding: The authors are thankful to the Deanship of Scientific Research at Najran University for funding this work under the Research Priorities and Najran Research funding program grant code NU/NRP/MRC/12/37.

Abstract

In this study, new series of N'-(2-(substitutedphenoxy)acetyl)-4-(1*H*-pyrrol-1-yl)benzohydrazides (**3a-j**) 4-(2,5-dimethyl-1*H*-pyrrol-1-yl)-N'-(2-(substitutedphenoxy)acetyl)benzohydrazides (**5a-j**) were synthesized, characterized and assessed as inhibitors of enoyl ACP reductase and DHFR. Most of the compounds exhibited dual inhibition against the enzymes enoyl ACP reductase and DHFR. Several synthesized substances also demonstrated significant antibacterial and antitubercular properties. A molecular docking analysis was conducted in order to determine the potential mechanism of action of the synthesized compounds. The results indicated that there were binding interactions seen with the active sites of dihydrofolate reductase and enoyl ACP reductase. Additionally, important structural details were identified that play a critical role in sustaining the dual inhibitory activity. These findings were useful for the development of future dual inhibitors. Therefore, this study provided strong evidence that several synthesized molecules could exert their antitubercular properties at the cellular level through multi-target inhibition. By shedding light on the mechanisms through which these compounds exert their inhibitory effects, this research opens up promising avenues for the future development of dual inhibitors with enhanced antibacterial and antitubercular properties. The study's findings underscore the importance of multi-target approaches in drug design, providing a strong foundation for the design and optimization of novel compounds that can effectively target bacterial infections at the cellular level.

Competing interests: The authors have declared that no competing interests exist.

1. Introduction

Since it has been around for millennia and continues to be extremely contagious, tuberculosis (TB) is a serious threat to human health [1]. According to estimates, the TB bacteria infect almost a quarter of the world's population. 1.5 million People die from TB each year, which affects 10 million people worldwide. It ranks as one of the most lethal infectious diseases in the world [2]. The bacterium that causes TB, the *Mycobacterium tuberculosis* (Mtb) has a very impermeable cell wall and grows slowly in acid. *Mycobacterium tuberculosis* (Mtb) is classified as an opportunistic pathogen, capable of entering a dormant state among macrophages for extended periods of time. Subsequently, it can reactivate in persons with weakened immune systems, particularly those co-infected with the human immunodeficiency virus (HIV). The emergence and proliferation of extensively drug-resistant (XDR) and multi-drug-resistant (MDR) tuberculosis (TB) strains exacerbate the existing problem [3,4]. Isoniazid and rifampicin, two widely used medicines, are still ineffective against MDR-TB germs [5–7]. India, China, and the Russian Federation were responsible for the largest proportions of the world load, with India accounting for 27%, China accounting for 14%, and the Russian Federation accounting for 9% [8–11]. Therefore, there is an urgent medical need for the development of novel chemotypes that are safer, more effective, and work through a variety of pathways.

Numerous pharmaceutical compounds containing nitrogen heterocycles are presently undergoing clinical trials with the aim of treating TB [12]. Pyrroles are notable within this category due to their substantial antimycobacterial activity, as indicated by previous research [13]. The heterocyclic ring template pyrrole, which has a variety of pharmacophores, makes it possible to create a library of enormous lead compounds. The pyrroles-based lead analogue, LL3858 (Fig 1) [14], is presently undergoing phase IIa clinical investigations in India. Lupin Limited firstly revealed the MIC range for LL3858 against Mtb in 2004. It varied from 0.05 to 0.1 µg/mL.

A structural characteristic of the pyrrole ring with advantageous electron characteristics is probably the cause of the improved interaction with enzymes and receptors. To attain the ideal activity profile, this element in the scaffold provides potential for further modification. Further research revealed that compounds with pyrrole based core structures exhibited a range of biological activities, including antimicrobial [15], antiviral [16], anticancer [17], and antimycobacterial [18–20] properties.

Dihydrofolate reductase (DHFR) catalyzes the reduction of dihydrofolate to tetrahydrofolate which couples with thymidylate synthase in the reductive methylation of deoxyuridine to deoxythymidine. Tetrahydrofolate cofactor deficiencies brought on by the suppression of DHFR function result in cell death. As a key target for the development of chemotherapeutic agents against bacterial and parasite diseases as well as TB, DHFR inhibition has long been recognized. Methotrexate and trimethoprim are examples of DHFR inhibitors used in the clinic.

Fatty acid production inhibition is a desirable target for the rational creation of novel antitubercular drugs among the various *Mycobacteria* targets being investigated for antitubercular action. The main element of the cell wall of Mtb is mycolic acid. For the development of new antimycobacterial drugs, fatty acid biosynthesis-related enzymes are regarded as the optimal targets. The fatty acid synthase enzymes FAS-I and FAS-II catalyse the production of fatty acids. In mammals, FAS-I catalyses the synthesis; in *Mycobacterium*, FAS-I and FAS-II do the catalyzing. Due to this distinction, FAS-II is a desirable target for the development of antitubercular drugs. The FAS-II system contains an essential enzyme known as enoyl-ACP (CoA) reductase (FabI/ENR/InhA) [21]. Isoniazid, the most recommended anti-tubercular drug, targets the inhA structural gene in Mtb as its main target. An enoyl-ACP (CoA) reductase with the specificity for chain elongation in mycolic acid precursors, InhA, was discovered [22].

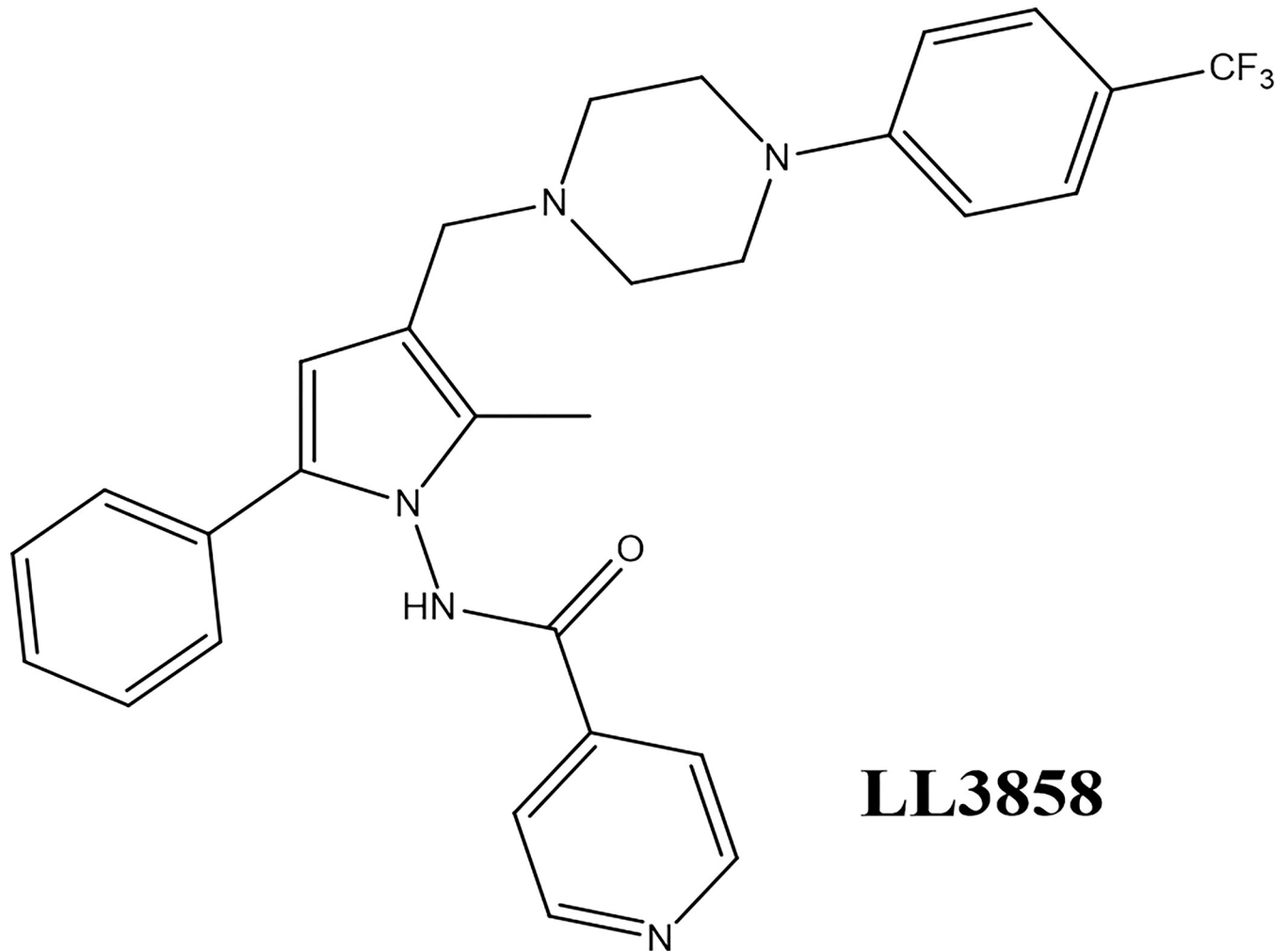


Fig 1. The potent antimycobacterial pyrrole analogue-LL3858.

<https://doi.org/10.1371/journal.pone.0303173.g001>

Different classes of direct inhibitors of InhA enzyme were investigated such as Triclosan and derivatives, GEQ analogues etc.

Our laboratory for Novel Drug Design and Discovery has been conducting research on the potential of DHFR and enoyl-ACP reductase as molecular targets for antitubercular therapies. Specifically, we have been investigating the use of pyrrole pharmacophoric scaffolds that inhibit both DHFR and enoyl-ACP reductase. The aim of our research is to develop novel compounds that can effectively inhibit both targets, thereby exhibiting antitubercular effects.

We have reported the synthesis of pyrrole compounds as antitubercular drugs and enoyl ACP reductase inhibitors in the prior studies [23–26].

In this study, we present the design and synthesis of 20 bioactive pyrrole scaffold-containing dual-target inhibitors of DHFR and enoyl-ACP reductase. Such inhibitors could get around the toxicity, drug-drug interactions, and/or pharmacokinetic drawbacks of using two different medications in combination chemotherapy treatments. Additionally, the price of a single medication may be less than the cost of two different treatments, and it may also increase patient compliance.

2. Results and discussion

According to the methodology described in Scheme 1, the target compounds, specifically 4-(1*H*-pyrrol-1-yl)-*N'*-(2-(substitutedphenoxy)acetyl)benzohydrazides (3a-j) and 4-(2,5-dimethyl-1*H*-pyrrol-1-yl)-*N'*-(2-(substitutedphenoxy)acetyl)benzohydrazides (5a-j), were synthesized (Fig 2). This synthesis involved the reaction of 4-pyrrol-1-yl benzoic acid hydrazide 2 or 4-(2,5-dimethyl pyrrol-1-yl)benzohydrazide 4 with substituted phenoxy acetic acids in distilled *N,N'*-dimethyl formamide. The reaction was facilitated by the coupling agent 2-(1*H*-benzotriazol-1-yl)-1,1,3,3-tetramethyluronium hexafluorophosphate and *N,N'*-diisopropylethylamine, which acted as a catalytic agent. The reaction was carried out under cold conditions. The structural confirmation of newly reported pyrrolyl-benzohydrazides was achieved by the analysis of spectral data.

In the ¹H NMR spectrum of compound 3d, proton of two -NH appeared as singlets at 10.49 and 10.14 δ ppm, two protons of phenyl-C₈, C₁₀ and two protons of bridging phenyl-C₇, C₁₁ appeared as two doublets at 8.02 δ and 7.76 δ ppm. Similarly, two protons of pyrrole-C₂, C₅ and two protons of phenyl-C₂₂, C₂₄ appeared as two doublets at 7.51 δ and 7.04 δ ppm respectively. The proton signals of pyrrole-C₃ and C₄ were observed as a triplet at a chemical shift range of 6.33–6.32 δ ppm, while the six methyl protons were observed as a singlet at a chemical shift of 2.22 δ ppm. The identification of the CH₂ group was confirmed by the observation of a singlet signal at 4.65 δ ppm. The ¹³C nuclear magnetic resonance (NMR) spectrum of

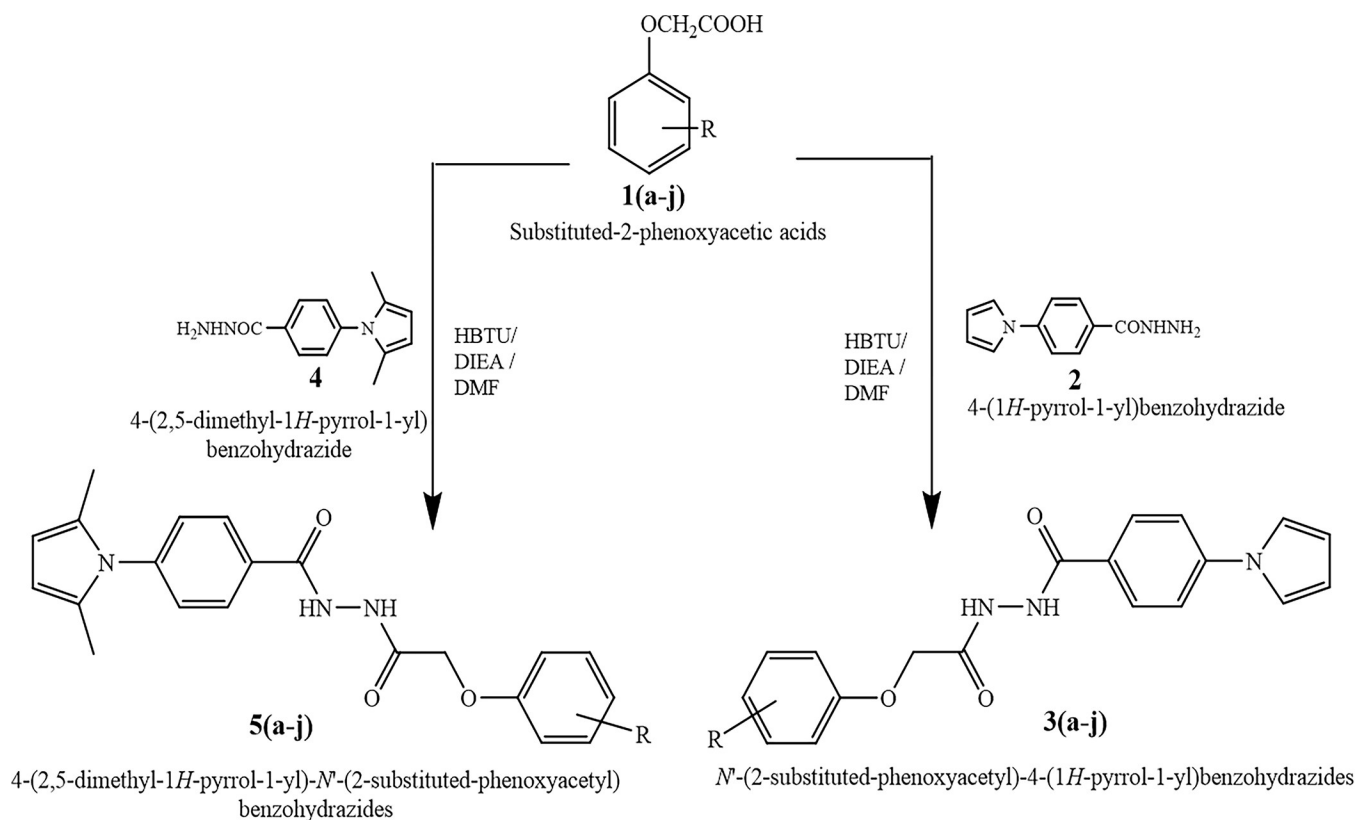


Fig 2. The scheme-1 outlines a synthetic pathway for the production of innovative derivatives of pyrrolyl-benzohydrazides.

<https://doi.org/10.1371/journal.pone.0303173.g002>

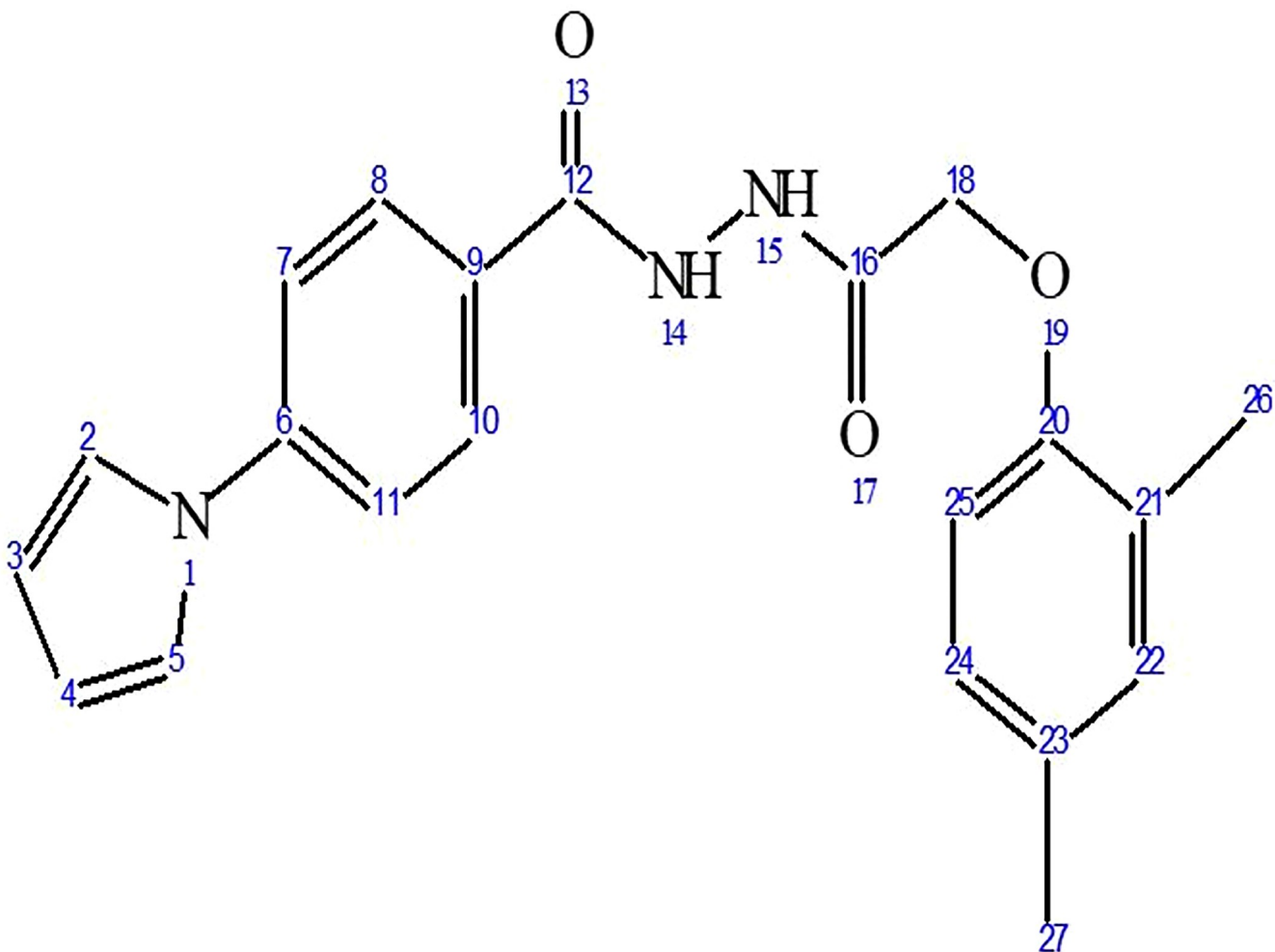


Fig 3. The compound 3d- structural confirmation.

<https://doi.org/10.1371/journal.pone.0303173.g003>

compound **3d** exhibited distinct peaks at 167.44 and 164.61 δ ppm, indicating the presence of two different carbonyl groups. Additionally, shifts corresponding to pyrrole and phenyl carbons were observed throughout the estimated range of δ ppm from 111.19 to 142.27. Moreover, the compound **3d**- structural confirmation was achieved through the examination of its mass spectrum. This analysis revealed a peak at m/z 365.26 ($M^+ + 2$), which corresponds to the compound's molecular weight calculated from expected molecular formula (Fig 3).

2.1. Molecular docking

The active pocket was found to be the area of the complex between the 2NSD_ligand and the 2NSD enoyl-ACP reductase. It was re-docked in order to get the contacts and orientation of the 2NSD_ligand at the active site for comparison with other synthesized compounds (Fig 4A and 4B). The synthetic molecule **3g** binds to the same binding site as 2NSD_ligand, according to the Surflex-Dock docking studies. The oxygen of the carbonyl group in the 2NSD_ligand has shown two H-bond interactions, creating two hydrogen bonds with the OH of the active sites of NAD⁺ ribose (2.06) and TYR158 (1.87) (Fig 5A and 5B). With the amino acid Tyr 158 and the co-factor NAD⁺, respectively, the oxygen atom of the carbonyl group has formed two

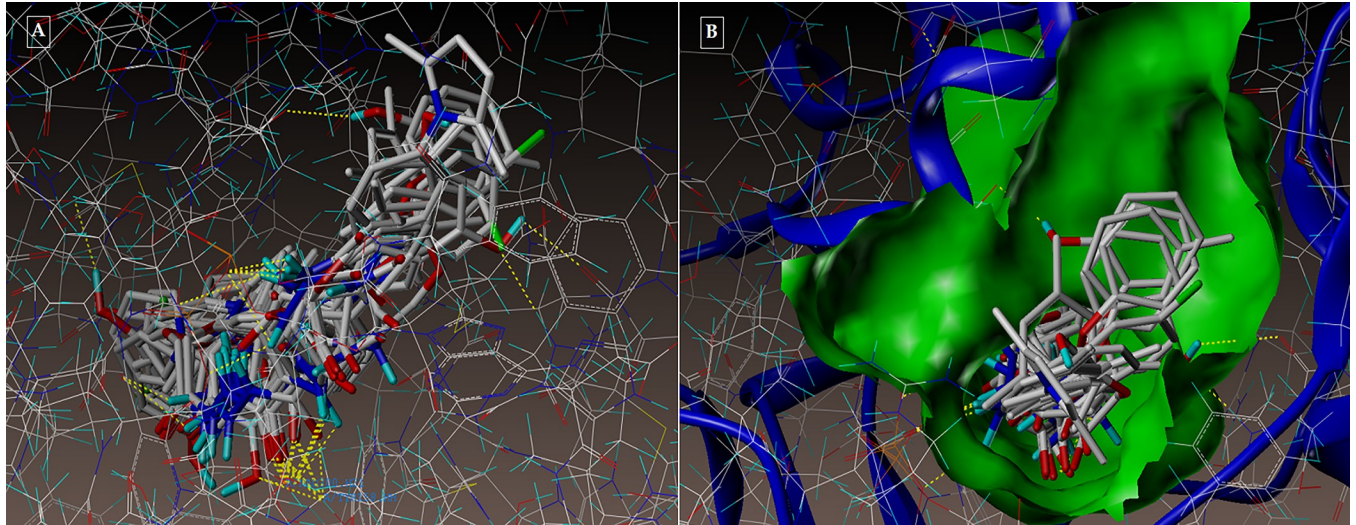


Fig 4. (A-B): Depicting the docked mode of all the compounds within the hypothesized binding pocket of InhA, as represented by PDB: 2NSD.

<https://doi.org/10.1371/journal.pone.0303173.g004>

H-bonding connections in the molecules **3g** and **5d** (Figs 6A, 6B, 7A and 7B). Fig 8A and 8B depict the hydrophobic and hydrophilic amino acids that are encircled by the two compounds **3g** and **5d**.

The consensus scores obtained for the compounds, which varied from 8.74 to 5.38, highlight the essentiality of all intermolecular interactions between the ligands and the InhA protein. The electrostatic and van der Waals forces between the protein and ligands exhibited a range of values spanning from -150.08 to -139.12. The Helmholtz free energies of interactions for atom pairs between proteins and ligands exhibited a range of values from -63.09 to -39.60. Additionally, the energies associated with H-bonding, complex formation between the ligand and protein, and internal interactions within the ligand itself ranged from -250.95 to -212.47. Furthermore, values ranging from -46.92 to -32.70 were observed for the ligands, indicating

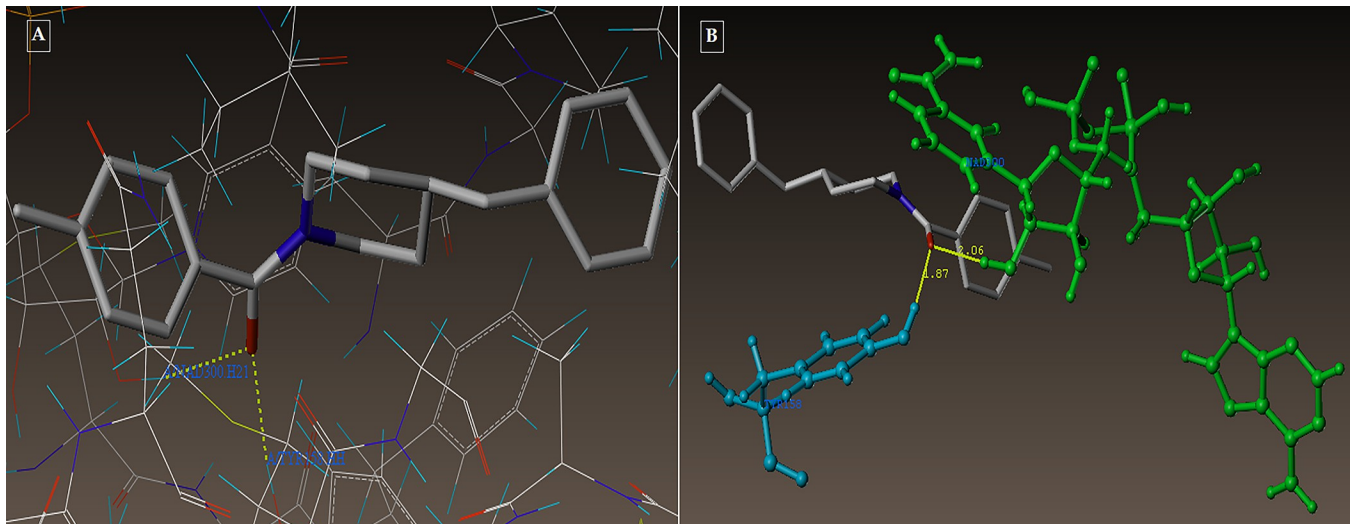


Fig 5. (A-B): depicting the 2NSD_ligand docked mode at InhA (A) and 2NSD_ligand 3D docked view (B). Tyr 158, a residue at the binding site, is colored cyan, NAD⁺ is colored green, and the molecule is colored according to the type of atom.

<https://doi.org/10.1371/journal.pone.0303173.g005>

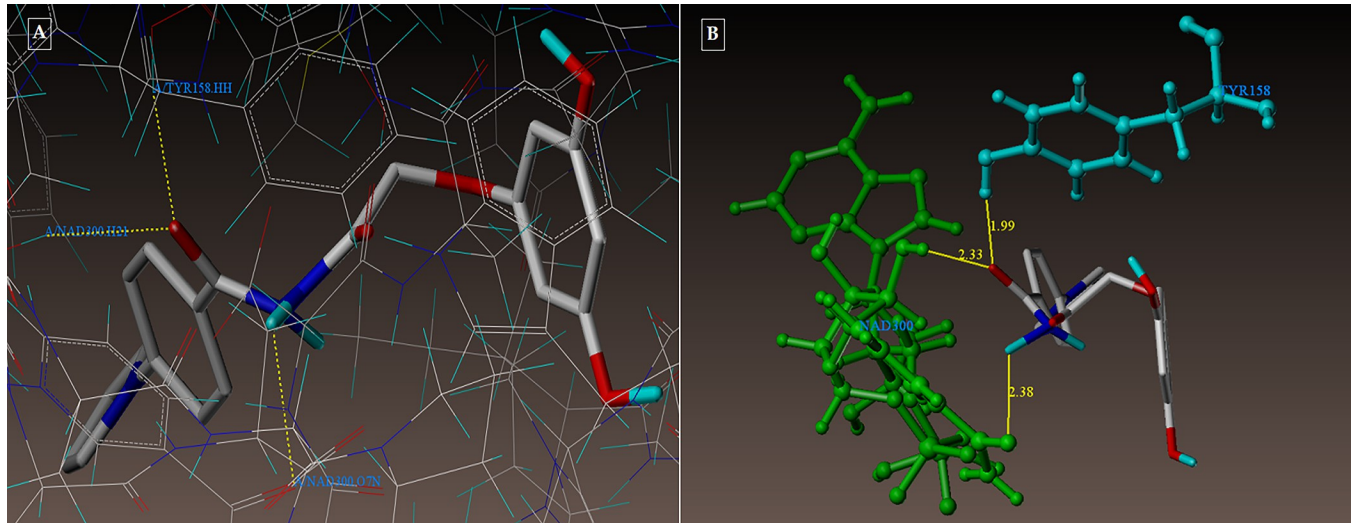


Fig 6. (A-B): (A) Compound 3g docked mode; (B) 3D docked view of the compound 3g. Binding site residues are cyan-colored Tyr 158 amino acid, green-colored co-factor NAD⁺, and the molecule is colored by atom type.

<https://doi.org/10.1371/journal.pone.0303173.g006>

the presence of H-bonding, lipophilic contact, and rotational entropy. The compounds have a preferential binding affinity towards InhA, as indicated by the observed outcomes and supporting references. The 2NSD ligand is a molecule that binds to a specific receptor or protein (Table 1).

All of the compounds had excellent docking scores (Fig 9A and 9B) against the dihydrofolate reductase forms of Mycobacterium TB, according to a second docking investigation using PDB ID: 1DF7.

Compound 3g forms three hydrogen bonding contacts at the enzyme's active site, as depicted in Fig 9A and 9B (PDB ID: 1DF7). ARG60's hydrogen atom is involved in one hydrogen bond raised by the oxygen of the benzohydrazide's C = O group (-O—H-ARG60, 2.12 Å),

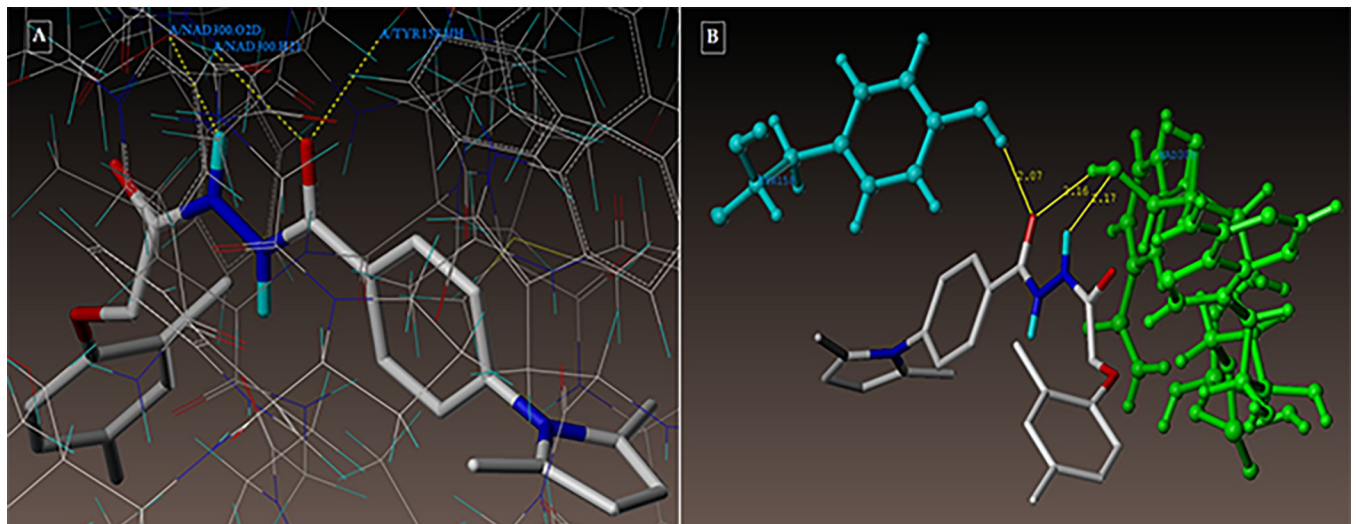


Fig 7. (A-B): (A) Compound 5d in docked mode; (B) Compound 5d in 3D docked view. Tyr 158, a residue at the binding site, is colored cyan, NAD⁺ is colored green, and the molecule is colored according to the type of atom.

<https://doi.org/10.1371/journal.pone.0303173.g007>

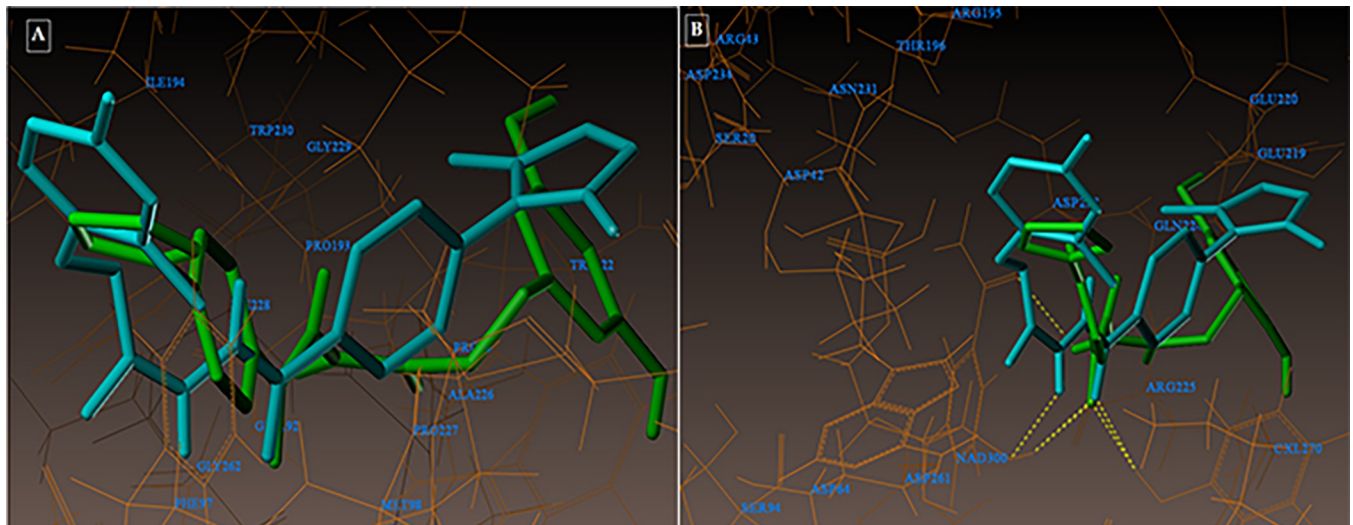


Fig 8. (A-B): depicting the hydrophobic and hydrophilic amino acids surrounding the compounds **3g** and **5d** under consideration.

<https://doi.org/10.1371/journal.pone.0303173.g008>

while GLN28's oxygen atom is involved in another (-H—O—GLN28 , 2.19 Å) by the NH group. As seen in Fig 10A and 10B (PDB ID: 1DF7), compound **5d** creates three hydrogen bonds in the enzyme's active site. These bonds are formed by the hydrogen atoms of ARG60 and ARG32 with the oxygen atom of the benzohydrazide's C = O group (-O—H—ARG60 , 2.10 Å, 2.13; O—H—ARG32 , 2.53 Å). The docked picture of the binding interaction of 1DF7_ligand (methotrexate) with enzyme active sites in Figs 11, 12A and 12B) shows 14 bonding connections. Fig 13A and 13B depict the hydrophobic and hydrophilic amino acids that are encircled by the two compounds **3g** and **5d**.

Table 2 provides a comprehensive summary of the intermolecular forces governing the interaction between ligands and the enzyme. It is noteworthy that all the compounds examined in this study had consensus scores ranging from 7.32 to 5.17. We also noticed that the examined compounds interacted with the amino acid residues (ARG60, ARG32, and GLN28) similarly to the 1DF7_ligand. This implies that molecules engage in comparable interactions with enzymes as ligands do.

2.2. Antitubercular and antibacterial activities

The findings of the antimicrobial study conducted on *S. aureus* (Gram-positive) and *E. coli* (Gram-negative) are presented in Table 3, as well as the results of the antitubercular testing of all substances against the *M. tuberculosis* H37Rv strain utilizing the MABA method. Its acronym is MIC, and it is used to describe a compound's specific activities. The compounds displayed good antitubercular activity between 1.6 and 12.5 µg/ml, according to the preliminary antitubercular studies. At MIC 3.12 µg/ml, compounds **3c**, **3d**, **3g**, **3h**, **5f**, **5g**, **5h**, and **5j** displayed greater activity. At MIC 1.6 µg/ml, compounds **5d** and **5e** exhibited the highest level of activity. Compounds shown antibacterial activity (given as MIC) between 1.6 and 100 µg/ml.

2.3. MtDHFR inhibitory activity

By observing the fluorescence given off by MtDHFR substrates when stimulated at 340 nm, the *in vitro* MtDHFR inhibitory activity of our newly synthesized compounds was determined (Table 3). Since the product (NADP⁺) is not luminescent, the enzyme's activity was evaluated

Table 1. Surflex Docking score in kcal/mol for pyrrole derivatives on the PDB ID: 2NSD.

| Compounds | Total Score ^a | Crash Score ^b | Polar Score ^c | D score ^d | PMF Score ^e | G Score ^f | Chem Score ^g |
|-------------|--------------------------|--------------------------|--------------------------|----------------------|------------------------|----------------------|-------------------------|
| 2NSD_ligand | 9.25 | -0.93 | 1.54 | -150.083 | -63.091 | -250.959 | -46.922 |
| 3g | 8.74 | -1.25 | 1.05 | -146.022 | -27.104 | -225.371 | -37.314 |
| 5d | 8.49 | -2.04 | 1.70 | -149.781 | -87.633 | -280.534 | -42.817 |
| 3a | 8.41 | -1.27 | 1.93 | -133.435 | -75.786 | -254.546 | -37.520 |
| 3h | 7.36 | -1.77 | 1.88 | -161.388 | -75.365 | -260.265 | -39.781 |
| 3i | 7.33 | -1.40 | 3.39 | -126.626 | -87.862 | -199.298 | -37.617 |
| 5g | 7.20 | -1.32 | 2.98 | -152.376 | -72.938 | -232.286 | -42.754 |
| 3e | 7.20 | -1.43 | 1.92 | -128.682 | -73.370 | -236.563 | -37.357 |
| 3b | 7.17 | -1.75 | 1.74 | -132.318 | -76.891 | -255.492 | -36.836 |
| 3c | 7.03 | -1.60 | 1.36 | -136.394 | -89.992 | -246.311 | -40.328 |
| 3d | 6.82 | -1.25 | 1.69 | -157.030 | -67.521 | -254.255 | -41.866 |
| 5e | 6.73 | -1.57 | 2.18 | -134.748 | -87.875 | -215.834 | -32.587 |
| 3f | 6.61 | -0.97 | 0.99 | -132.540 | -70.899 | -222.874 | -36.092 |
| 5f | 6.56 | -1.20 | 2.09 | -149.617 | -68.155 | -231.933 | -43.693 |
| 3c | 6.50 | -1.50 | 1.96 | -127.158 | -82.426 | -220.411 | -35.503 |
| 5c | 6.32 | -1.78 | 0.61 | -144.670 | -41.953 | -269.401 | -33.218 |
| 5i | 6.27 | -1.32 | 1.95 | -117.248 | -68.432 | -203.390 | -30.528 |
| 5h | 6.23 | -1.66 | 0.03 | -145.411 | -36.648 | -218.277 | -33.512 |
| 5b | 6.18 | -1.30 | 1.86 | -149.846 | -68.844 | -233.856 | -40.982 |
| 5c | 6.10 | -2.41 | 1.75 | -145.601 | -35.947 | -248.880 | -38.471 |
| 5a | 5.38 | -1.92 | 0.10 | -139.123 | -39.609 | -212.476 | -32.706 |

^aCScore The Consensus Score algorithm combines various widely used scoring algorithms to rank the affinity of ligands that are coupled to the active site of a receptor. It then provides the overall score as the output.

^bCrash-score- The crash-score reveals the improper penetration into the binding point. Crash scores close to 0 are considered positive. Penetration is indicated by negative values.

^cPolar- denotes the contribution of polar interactions to the overall score. The polar score may be beneficial for filtering out docking findings that do not form any hydrogen bonds.

^dD-score- Charge and van der Waals interactions between the protein and the ligand are given a D-score.

^ePMF-score- The Helmholtz free energy of interactions for protein-ligand atom pairs are indicated by the PMF-score (Potential of Mean Force, PMF).

^fG-score- The G-score demonstrates hydrogen bonding, complex (ligand-protein), and internal (ligand-ligand) energies.

<https://doi.org/10.1371/journal.pone.0303173.t001>

by consuming its substrate. Trimethoprim, the assay's positive control, had an IC₅₀ value of 92 μM using this method, which was consistent with the findings from the literature (88 μM). **Table 3** shows that the majority of the investigated compounds were much more effective against MtDHFR. Six of them (**3c**, **3d**, **3g**, **3h**, **5d**, and **5e**) had greater inhibition characteristics than trimethoprim.

2.4. ADME studies

The Swiss ADME web tool calculated the ADME properties of every synthesised compound, and every molecule complies with Lipinski's rule of five. All compounds have good synthetic accessibility, moderate solubility, and GI absorption, according to Swiss ADME tests. The BBB is only not crossed by compounds **3c**, **3g**, **3i**, **5c**, **5g** and **5i**. The substances had skin permeability that ranged from -5.61 to -7.06, which was moderate. **Table 4** presents the outcomes.

ProTox-II determined the toxicological summaries of all the chemicals, and **Table 5** shows the toxic effects. This data on toxicity demonstrated that none of the molecules shown any toxicity.

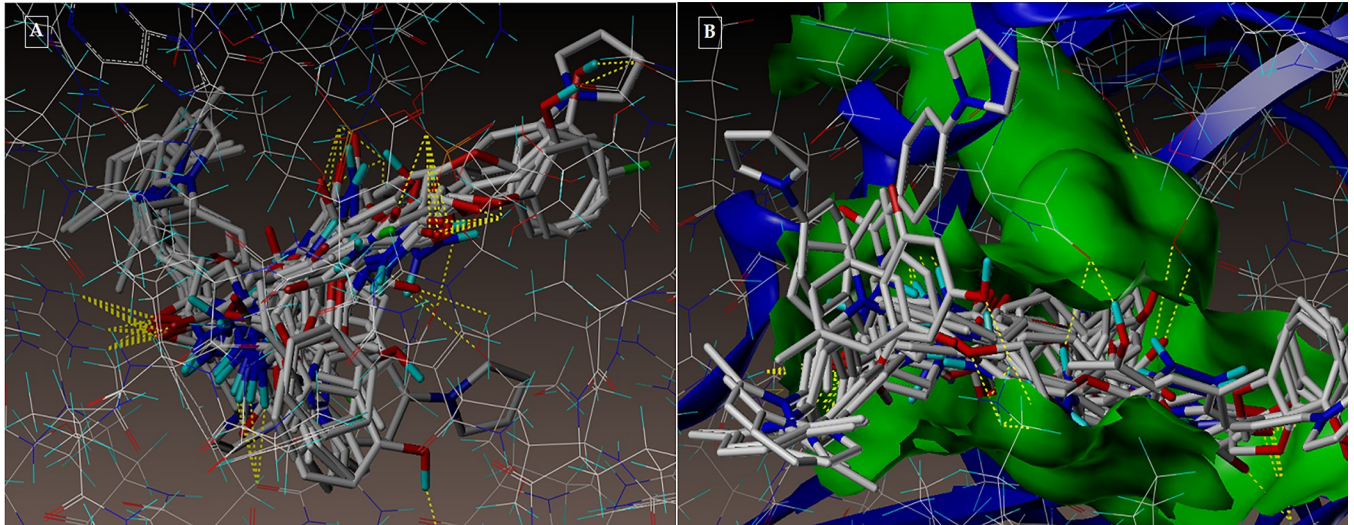


Fig 9. (A-B): The docking mechanism of all the synthesized compounds within the proposed binding pocket of InhA (PDB: 1DF7).

<https://doi.org/10.1371/journal.pone.0303173.g009>

The study explores pyrrole-based compounds that act as dual inhibitors and their impact on current tuberculosis (TB) treatment, especially in relation to resistance mechanisms. TB is a significant global health issue, and the development of drug-resistant strains presents a significant obstacle to successful treatment. Approaching this challenge involves targeting multiple essential enzymes involved in the survival and replication of *M. tuberculosis*, the bacterium responsible for TB [14,19].

Dual inhibitors offer a significant advantage by targeting two distinct enzymes, enoyl ACP reductase and DHFR, essential for bacterial growth. By inhibiting both enzymes, dual inhibitors disrupt multiple metabolic pathways, making it more challenging for the bacterium to develop resistance through mutations in a single target.

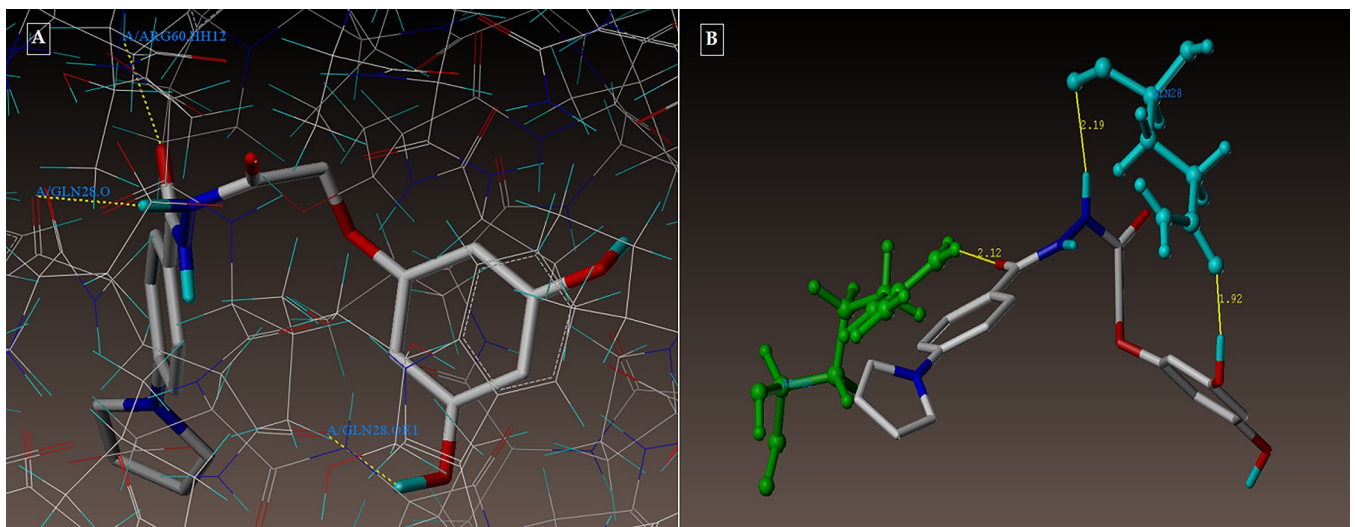


Fig 10. (A-B): (A) Compound 3g docked mode; (B) Compound 3g 3D-docked view. Binding site residues include cyan-colored GLN28 amino acids, green-colored ARG60 amino acids, and a molecule that is colored according to atom type.

<https://doi.org/10.1371/journal.pone.0303173.g010>

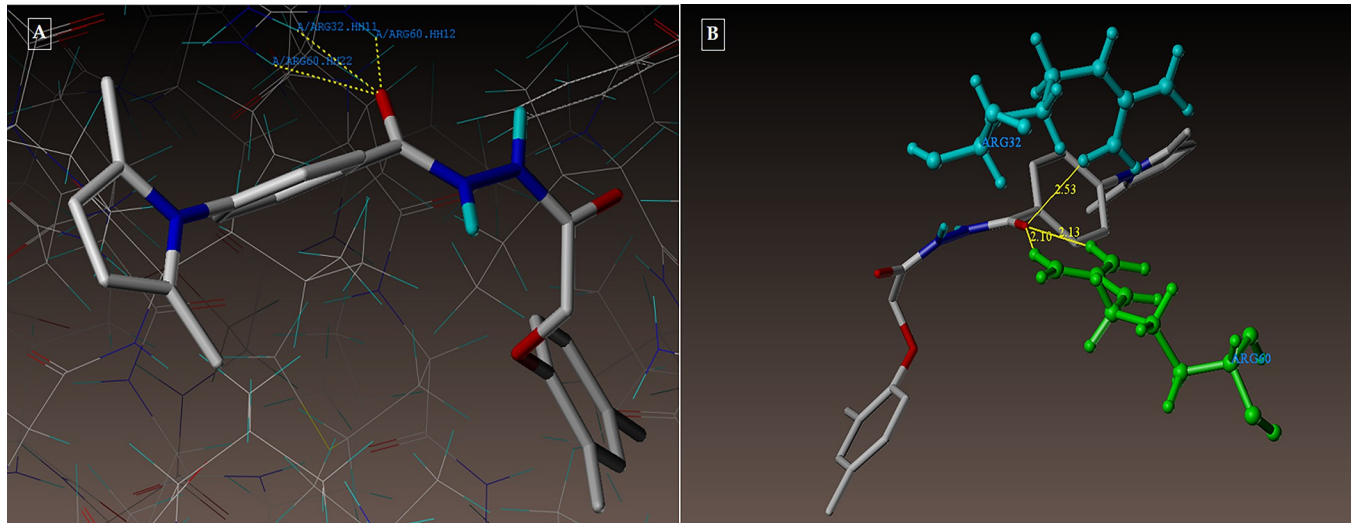


Fig 11. (A-B): (A) Compound 5d docked mode; (B) Compound 5d 3D-docked view. Binding site residues: cyan ARG32 amino acid, green ARG60, and the molecule is colored according to atom type.

<https://doi.org/10.1371/journal.pone.0303173.g011>

Resistance mechanisms in TB usually result from mutations in the genes that encode the targeted enzymes, resulting in decreased drug binding affinity or changed enzyme activity. Using dual inhibitors can be beneficial in addressing resistance by providing a stronger defense against resistance development. Changes that provide resistance to one enzyme may not necessarily provide resistance to the other enzyme targeted by the dual inhibitor. By using this approach, the chances of the bacterium becoming resistant to the combination therapy are minimized, which could be a successful method to address drug-resistant strains [14,27].

In addition, the study's molecular docking analysis offers valuable information on how the synthesized compounds interact with the active sites of enoyl ACP reductase and DHFR. By comprehending these interactions, we are able to guide the design and enhancement of upcoming dual inhibitors with improved effectiveness and specificity. Researchers have

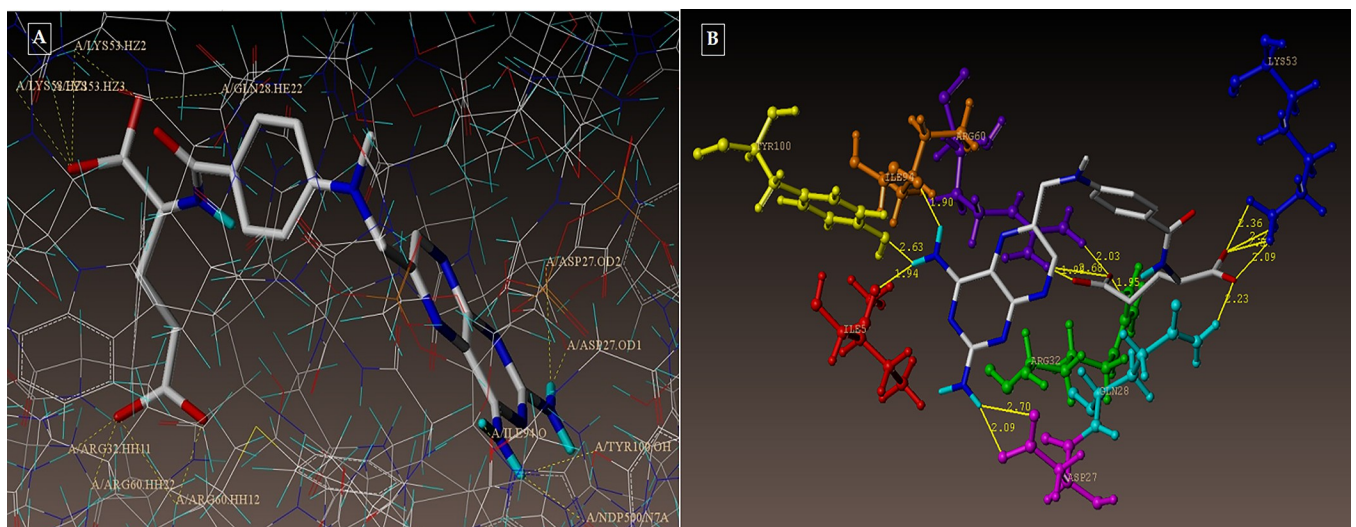


Fig 12. (A-B): (A) 1DF7_ligand docked mode at InhA; (B) 3D-Docked view of 1DF7_ligand.

<https://doi.org/10.1371/journal.pone.0303173.g012>

Table 3. Newly synthesized pyrrole compounds' preliminary *in vitro* antibacterial, antitubercular, MtDHFR, and enoyl ACP reductase inhibition values.

| Compound | <i>M. tuberculosis</i> H ₃₇ Rv MIC values in $\mu\text{g ml}^{-1}$ | <i>S. aureus</i> (Gram +ve) | <i>E. coli</i> (Gram-ve) | IC ₅₀ (μM) MtDHFR | % Inhibition of InhA at 50 μM |
|---------------|---|-----------------------------|--------------------------|--|--|
| | | MIC ($\mu\text{g/mL}$) | MIC ($\mu\text{g/mL}$) | | |
| 3a | 12.5 (37.27) | 100 (298.18) | 6.25 (99.70) | - | - |
| 3b | 12.5 (35.77) | 100 (286.21) | 6.25 (17.88) | - | - |
| 3c | 3.12 (8.87) | 100 (284.60) | 3.12 (8.87) | 25 | 46 |
| 3d | 3.12 (8.58) | 100 (275.16) | 1.6 (4.40) | 32 | 48 |
| 3e | 6.25 (17.88) | 100 (286.21) | 12.5 (35.77) | - | - |
| 3f | 6.25 (16.90) | 100 (270.40) | 12.5 (33.80) | 122 | - |
| 3g | 3.12 (8.49) | 100 (272.21) | 1.6 (4.35) | 20 | 63 |
| 3h | 3.12 (8.58) | 100 (275.16) | 3.12 (8.58) | 19 | 59 |
| 3i | 12.5 (35.57) | 100 (284.60) | 12.5 (35.57) | - | - |
| 3j | 12.5 (33.80) | 100 (270.40) | 6.25 (16.90) | - | - |
| 5a | 6.25 (17.19) | 100 (275.16) | 6.25 (17.19) | 98 | 26 |
| 5b | 12.5 (33.11) | 100 (264.94) | 12.5 (33.11) | - | - |
| 5c | 12.5 (32.94) | 100 (263.56) | 12.5 (32.94) | - | - |
| 5d | 1.6 (4.09) | 100 (255.63) | 3.12 (7.97) | 56 | 62 |
| 5e | 1.6 (4.23) | 100 (264.94) | 3.12 (8.26) | 62 | 66 |
| 5f | 3.12 (7.84) | 100 (251.34) | 6.25 (15.70) | - | - |
| 5g | 3.12 (7.89) | 100 (252.89) | 3.12 (7.89) | - | - |
| 5h | 3.12 (7.6) | 100 (255.44) | 3.12 (7.6) | - | - |
| 5i | 6.25 (16.47) | 100 (263.56) | 3.12 (8.22) | - | - |
| 5j | 3.12 (7.84) | 100 (251.34) | 6.25 (15.70) | - | - |
| Pyrazinamide | 3.12 | - | - | - | - |
| Streptomycin | 6.25 | - | - | - | - |
| Ciprofloxacin | - | 2 | 2 | - | - |
| TMP | - | - | - | 92 | - |
| TCL | - | - | - | - | >99 |

Results are expressed as % InhA inhibition.

<https://doi.org/10.1371/journal.pone.0303173.t003>

the groundwork for creating new compounds with improved antibacterial and antitubercular properties.

3. Experimental section

3.1. Chemicals

Chemicals were procured from Spectrochem Pvt Ltd, Sigma Aldrich, and S. D. Fine Chem. Ltd for the purpose of synthesizing the mentioned compounds. Both the recrystallization procedure and the distillation method were employed for the purification of various compounds and solvents.

3.2. Instruments

The synthesized compounds' melting points were determined using the SHITAL-Digital programmable melting point apparatus (SSI-22(B)) and occasionally with the Thiles Tube. These values are reported without any corrections. Infrared spectra were acquired using KBr pellets on the Bruker-T spectrophotometer. The chemical shifts in this study were quantified in terms of δ values (parts per million) for both the ¹H NMR and ¹³C NMR analyses. These measurements were conducted using Bruker Avance IINMR400/100 MHz equipment, with

Table 4. Swiss ADME web tool's ADME properties for synthetic molecules.

| Compound | Log P | Molar refractivity | TPSA | HBA | HBD | RB | GI Absorption | BBB Permeant | Log Kp cm/s | Solubility | CYP inhibitor | | | | | Lipinski violation | Synthetic accessibility |
|----------|-------|--------------------|--------|-----|-----|----|---------------|--------------|-------------|--------------------|---------------|------|-----|-----|-----|--------------------|-------------------------|
| | | | | | | | | | | | 1A2 | 2C19 | 2C9 | 2D6 | 3A4 | | |
| 3a | 2.48 | 92.59 | 72.36 | 3 | 2 | 8 | High | Yes | -6.36 | Soluble | No | Yes | Yes | Yes | No | 0 | 2.43 |
| 3b | 2.53 | 97.55 | 72.36 | 3 | 2 | 8 | High | Yes | -6.18 | Soluble | No | Yes | Yes | Yes | Yes | 0 | 2.55 |
| 3c | 1.47 | 94.61 | 92.59 | 4 | 3 | 8 | High | No | -6.70 | Soluble | No | No | No | Yes | No | 0 | 2.53 |
| 3d | 2.78 | 102.52 | 72.36 | 3 | 2 | 8 | High | Yes | -6.01 | Moderately Soluble | No | Yes | Yes | Yes | Yes | 0 | 2.75 |
| 3e | 2.75 | 97.55 | 72.36 | 3 | 2 | 8 | High | Yes | -6.18 | Soluble | Yes | Yes | Yes | Yes | Yes | 0 | 2.56 |
| 3f | 2.96 | 97.60 | 72.36 | 3 | 2 | 8 | High | Yes | -6.12 | Moderately Soluble | Yes | Yes | Yes | Yes | Yes | 0 | 2.48 |
| 3g | 1.89 | 96.63 | 112.82 | 5 | 4 | 8 | High | No | -7.06 | Soluble | No | No | No | Yes | No | 0 | 2.60 |
| 3h | 2.92 | 102.52 | 72.36 | 3 | 2 | 8 | High | Yes | -6.01 | Moderately Soluble | No | Yes | Yes | Yes | Yes | 0 | 2.68 |
| 3i | 1.63 | 94.61 | 92.59 | 4 | 3 | 8 | High | No | -6.70 | Soluble | No | No | No | Yes | No | 0 | 2.57 |
| 3j | 2.55 | 97.60 | 72.36 | 3 | 2 | 8 | High | Yes | -6.12 | Moderately Soluble | Yes | Yes | Yes | Yes | Yes | 0 | 2.57 |
| 5a | 2.56 | 102.52 | 72.36 | 3 | 2 | 8 | High | Yes | -5.95 | Moderately Soluble | No | Yes | Yes | Yes | Yes | 0 | 2.74 |
| 5b | 2.77 | 107.28 | 72.36 | 3 | 2 | 8 | High | Yes | -5.78 | Moderately Soluble | No | Yes | Yes | Yes | Yes | 0 | 2.85 |
| 5c | 2.33 | 104.54 | 92.59 | 4 | 3 | 8 | High | No | -6.31 | Moderately Soluble | No | No | Yes | Yes | No | 0 | 2.83 |
| 5d | 3.62 | 112.45 | 72.36 | 3 | 2 | 8 | High | Yes | -5.61 | Moderately Soluble | No | Yes | Yes | Yes | Yes | 0 | 3.05 |
| 5e | 2.66 | 107.48 | 72.36 | 3 | 2 | 8 | High | Yes | -5.78 | Moderately Soluble | No | Yes | Yes | Yes | Yes | 0 | 2.87 |
| 5f | 3.21 | 107.53 | 72.36 | 3 | 2 | 8 | High | Yes | -5.72 | Moderately Soluble | Yes | Yes | Yes | Yes | Yes | 0 | 2.77 |
| 5g | 2.62 | 106.56 | 112.82 | 5 | 4 | 8 | High | No | -6.65 | Moderately Soluble | Yes | No | Yes | Yes | No | 0 | 2.90 |
| 5h | 3.24 | 112.45 | 72.36 | 3 | 2 | 8 | High | Yes | -5.61 | Moderately Soluble | No | Yes | Yes | Yes | Yes | 0 | 2.99 |
| 5i | 2.65 | 104.54 | 92.59 | 4 | 3 | 8 | High | No | -6.31 | Moderately Soluble | No | No | Yes | Yes | No | 0 | 2.86 |
| 5j | 2.74 | 107.53 | 72.36 | 3 | 2 | 8 | High | Yes | -5.72 | Moderately Soluble | No | Yes | Yes | Yes | Yes | 0 | 2.86 |

<https://doi.org/10.1371/journal.pone.0303173.t004>

dimethylsulfoxide (DMSO-d₆) serving as the solvent and tetramethylsilane (TMS) used as the internal standard. The nuclear magnetic resonance (NMR) spectra can be categorized into several signal patterns, including singlet (s), doublet (d), doublet of doublet (dd), triplet (t), quartet (q), and multiplet (m). The mass spectra of all the compounds obtained with the MS-Waters SynaptG2 instrument exhibited data that was consistent with the anticipated molecular structure. The experimental procedure involved the implementation of analytical thin layer chromatography (TLC) utilizing Silica Gel GF as the stationary phase, while the mobile phase's progression was monitored through the utilization of an ultraviolet lamp.

3.3. General procedure for the synthesis of pyrrolylbenzohydrazide derivatives 3(a-j) and 5(a-j)

4-pyrrol-1-yl benzoic acid hydrazide 2/ 4-(2,5-dimethyl pyrrol-1-yl)benzohydrazide 4 [29] (0.0018 mol) was dissolved in 20 ml of dry DMF. Subsequently, in a low temperature

Table 5. Toxicity studies of synthesized compounds.

| Compound code | LD50 mg/kg | Hepatotoxicity | Carcinogenicity | Immunotoxicity | Mutagenicity | Cytotoxicity | Aryl hydrocarbon Receptor | Androgen Receptor (AR) | Androgen Receptor Ligand Binding Domain | Aromatase | Estrogen Receptor Ligand Binding Domain | Peroxisome Proliferator Activated Receptor Gamma | Nuclear factor | Heat shock factor response element | Mitochondrial Membrane Potential | Phosphoprotein | ATPase family AAA domain containing protein 5 |
|---------------|------------|----------------|-----------------|----------------|--------------|--------------|---------------------------|------------------------|---|-----------|---|--|----------------|------------------------------------|----------------------------------|----------------|---|
| 3a | 400 | Active | Active | Inactive | Inactive | Inactive | Inactive | Inactive | Inactive | Inactive | Inactive | Inactive | Inactive | Inactive | Inactive | Inactive | Inactive |
| 3b | 400 | Active | Active | Inactive | Inactive | Inactive | Inactive | Inactive | Inactive | Inactive | Inactive | Inactive | Inactive | Inactive | Inactive | Inactive | Inactive |
| 3c | 375 | Active | Inactive | Inactive | Inactive | Inactive | Inactive | Inactive | Inactive | Inactive | Inactive | Inactive | Inactive | Inactive | Inactive | Inactive | Inactive |
| 3d | 400 | Active | Active | Inactive | Inactive | Inactive | Inactive | Inactive | Inactive | Inactive | Inactive | Inactive | Inactive | Inactive | Inactive | Inactive | Inactive |
| 3e | 400 | Active | Active | Inactive | Inactive | Inactive | Inactive | Inactive | Inactive | Inactive | Inactive | Inactive | Inactive | Inactive | Inactive | Inactive | Inactive |
| 3f | 375 | Active | Inactive | Inactive | Inactive | Inactive | Inactive | Inactive | Inactive | Inactive | Inactive | Inactive | Inactive | Inactive | Inactive | Inactive | Inactive |
| 3g | 1000 | Active | Inactive | Inactive | Inactive | Inactive | Inactive | Inactive | Inactive | Inactive | Inactive | Inactive | Inactive | Inactive | Inactive | Inactive | Inactive |
| 3h | 400 | Active | Inactive | Inactive | Inactive | Inactive | Inactive | Inactive | Inactive | Inactive | Inactive | Inactive | Inactive | Inactive | Inactive | Inactive | Inactive |
| 3i | 1000 | Active | Inactive | Inactive | Inactive | Inactive | Inactive | Inactive | Inactive | Inactive | Inactive | Inactive | Inactive | Inactive | Inactive | Inactive | Inactive |
| 3j | 375 | Active | Inactive | Inactive | Inactive | Inactive | Inactive | Inactive | Inactive | Inactive | Inactive | Inactive | Inactive | Inactive | Inactive | Inactive | Inactive |
| 5a | 1600 | Active | Active | Inactive | Inactive | Inactive | Inactive | Inactive | Inactive | Inactive | Inactive | Inactive | Inactive | Inactive | Inactive | Inactive | Inactive |
| 5b | 1600 | Active | Inactive | Inactive | Inactive | Inactive | Inactive | Inactive | Inactive | Inactive | Inactive | Inactive | Inactive | Inactive | Inactive | Inactive | Inactive |
| 5c | 475 | Active | Inactive | Inactive | Inactive | Inactive | Inactive | Inactive | Inactive | Inactive | Inactive | Inactive | Inactive | Inactive | Inactive | Inactive | Inactive |
| 5d | 475 | Active | Inactive | Inactive | Inactive | Inactive | Inactive | Inactive | Inactive | Inactive | Inactive | Inactive | Inactive | Inactive | Inactive | Inactive | Inactive |
| 5e | 475 | Active | Inactive | Inactive | Inactive | Inactive | Inactive | Inactive | Inactive | Inactive | Inactive | Inactive | Inactive | Inactive | Inactive | Inactive | Inactive |
| 5f | 278 | Active | Inactive | Inactive | Inactive | Inactive | Inactive | Inactive | Inactive | Inactive | Inactive | Inactive | Inactive | Inactive | Inactive | Inactive | Inactive |
| 5g | 475 | Active | Inactive | Inactive | Inactive | Inactive | Inactive | Inactive | Inactive | Inactive | Inactive | Inactive | Inactive | Inactive | Inactive | Inactive | Inactive |
| 5h | 475 | Active | Inactive | Inactive | Inactive | Inactive | Inactive | Inactive | Inactive | Inactive | Inactive | Inactive | Inactive | Inactive | Inactive | Inactive | Inactive |
| 5i | 475 | Active | Inactive | Inactive | Inactive | Inactive | Inactive | Inactive | Inactive | Inactive | Inactive | Inactive | Inactive | Inactive | Inactive | Inactive | Inactive |
| 5j | 1700 | Active | Inactive | Inactive | Inactive | Inactive | Inactive | Inactive | Inactive | Inactive | Inactive | Inactive | Inactive | Inactive | Inactive | Inactive | Inactive |

<https://doi.org/10.1371/journal.pone.0303173.t005>

environment, a solution containing 0.0019 moles of substituted-2-phenoxy acetic acids (1a-j) was introduced. Hexafluorophosphate benzotriazole urea (HBTU) (0.87 grams, 0.0023 moles) and diisopropylethylamine (DIEA) (0.93 milliliters, 0.0053 moles) were introduced into the aforementioned combination and subjected to vigorous agitation for a duration of 24 to 30 hours at a temperature of 25°C. A solution containing 25% aqueous sodium chloride (NaCl) was employed to terminate the reaction, followed by the extraction of the resulting combination using ethyl acetate in three separate aliquots of 15 ml each. The ethyl acetate extract that was collected underwent a washing process using a saturated solution of Na₂CO₃ (20 ml) and 1N HCl (15 ml). Subsequently, a 10 ml solution of sodium chloride (NaCl) with a concentration of 25% was introduced into the procedure. After the ethyl acetate extract was dried using anhydrous sodium sulphate, it was concentrated using a rota-vapour. The resultant residue underwent purification by column chromatography, employing an eluent mixture of ethyl acetate and petroleum ether in a ratio of 6:4. The supplementary file contains all relevant spectra.

3.3.1. Synthesis of (3a): N²-(2-phenoxyacetyl)-4-(1H-pyrrol-1-yl) benzohydrazide.

White amorphous solid. (Yield 65%). M.p 138–140°C; FTIR (KBr-cm⁻¹): 3425 (NH), 3239 (NH), 2919 (Ar-C = CH), 1697 (C = O), 1652 (C = O).

¹H NMR (8 mg-DMSO-d₆, 400 MHz, T-18.85°C, δ ppm): 10.30 (1H, s, CONH), 10.26 (1H, s, NHCO), 8.00 (2H, d, *J* = 8.76 Hz, bridging phenyl-C₈, C₁₀-H), 7.78 (2H, d, *J* = 8.56 Hz, bridging phenyl-C₇, C₁₁-H), 7.51 (2H, d, *J* = 2.24 Hz, pyrrole-C₂, C₅-H), 7.35–7.30 (2H, m, phenyl-C₂₂, C₂₄-H), 7.05–6.90 (3H, m, phenyl-C₂₁, C₂₃, C₂₅-H), 6.32 (2H, d, *J* = 2.12 Hz, pyrrole-C₃, C₄-H), 4.69 (2H, d, *J* = 6.04 Hz, CH₂-H).

¹³C NMR (10 mg-DMSO-d₆, 400 MHz, T-18.85°C, δ ppm): 167.44 (-NHCO), 164.61 (-CONH), 156.58 (phenyl-C₂₀), 143.60 (bridging phenyl-C₆), 129.50 (bridging phenyl-C₈, C₁₀), 129.37 (bridging phenyl-C₇, C₁₁), 129.17 (phenyl-C₂₂, C₂₄), 127.67 (bridging phenyl-C₉), 121.33 (phenyl-C₂₃), 116.86 (pyrrole-C₂, C₅), 115.72 (phenyl-C₂₁, C₂₅), 106.18 (pyrrole-C₃, C₄), 66.58 (-CH₂).

Mass (ESI- *m/z*) = found 335.2440 [M⁺]; Calcd. 335.36.

CHN Anal. For C₁₉H₁₇N₃O₃: Calcd. C, 68.05; H, 5.11; N, 12.53; Found: C, 68.01; H, 5.04; N, 12.49.

3.3.2. Synthesis of (3b): 4-(1H-pyrrol-1-yl)-N²-(2-(p-tolyloxy)acetyl)benzohydrazide.

White amorphous solid. (Yield 59%). M.p 162–165°C; FTIR (KBr-cm⁻¹): 3381 (NH), 3239 (NH), 2922 (Ar-C = CH), 1691 (C = O), 1650 (C = O).

¹H NMR (8 mg-DMSO-d₆, 400 MHz, T-18.85°C, δ ppm): 10.21 (1H, s, CONH), 10.10 (1H, s, NHCO), 8.03 (2H, d, *J* = 8.32 Hz, bridging phenyl-C₈, C₁₀-H), 7.64 (2H, d, *J* = 8.28 Hz, bridging phenyl-C₇, C₁₁-H), 7.36 (2H, d, *J* = 7.04 Hz, pyrrole-C₂, C₅-H), 7.08 (2H, d, *J* = 10.44 Hz, phenyl-C₂₂, C₂₄-H), 6.92 (2H, d, *J* = 8.04 Hz, phenyl-C₂₁, C₂₅-H), 6.30 (2H, s, pyrrole-C₃, C₄-H), 4.61 (2H, s, CH₂-H), 2.24 (3H, s, CH₃-H).

¹³C NMR (10 mg-DMSO-d₆, 400 MHz, T-18.85°C, δ ppm): 167.29, (-NHCO), 164.89 (-CONH), 155.63 (phenyl-C₂₀), 141.30 (bridging phenyl-C₆), 129.99 (bridging phenyl-C₈, C₁₀), 128.49 (bridging phenyl-C₇, C₁₁), 127.91 (phenyl-C₂₂, C₂₄), 127.51 (bridging phenyl-C₉), 121.35 (phenyl-C₂₃), 116.71 (pyrrole-C₂, C₅), 114.58 (phenyl-C₂₁, C₂₅), 106.47 (pyrrole-C₃, C₄), 66.25 (-CH₂), 20.05 (-CH₃).

Mass (ESI- *m/z*) = Found 349.7444 [M⁺]; Calcd. 349.39.

CHN Anal. For C₂₀H₁₉N₃O₃: Calcd. C, 68.75; H, 5.48; N, 12.03; Found: C, 68.69; H, 5.41; N, 12.01.

3.3.3. Synthesis of (3c): N²-(2-(2-hydroxyphenoxy)acetyl)-4-(1H-pyrrol-1-yl)benzohydrazide. White amorphous solid. (Yield 75%). M.p 182–185°C; FTIR (KBr-cm⁻¹): 3402 (OH), 3398 (NH), 3279 (NH), 2924 (Ar-C = CH), 1681 (C = O), 1643 (C = O).

^1H NMR (8 mg-DMSO- d_6 , 400 MHz, T-18.85°C, δ ppm): 10.53 (1H, s, CONH), 10.45 (1H, s, NHCO), 9.00 (1H, s, OH), 8.03 (2H, d, $J = 8.76$ Hz, bridging phenyl-C₈, C₁₀-H), 7.77 (2H, d, $J = 8.80$ Hz, bridging phenyl-C₇, C₁₁-H), 7.52 (2H, d, $J = 2.24$ Hz, pyrrole-C₂, C₅-H), 7.04 (1H, d, $J = 7.56$ Hz, phenyl-C₂₂), 6.86–6.77 (3H, m, phenyl-C₂₃, C₂₄, C₂₅-H), 6.30 (2H, d, $J = 2.16$ Hz, pyrrole-C₃, C₄-H), 4.68 (2H, s, CH₂-H).

^{13}C NMR (10 mg-DMSO- d_6 , 400 MHz, T-18.85°C, δ ppm): 167.00 (-NHCO), 164.86 (-CONH), 146.14 (phenyl-C₂₁), 145.29 (phenyl-C₂₀), 142.34 (bridging phenyl-C₆), 129.15 (bridging phenyl-C₈, C₁₀), 128.49 (bridging phenyl-C₇, C₁₁), 122.15 (phenyl-C₂₂, C₂₄), 119.32 (bridging phenyl-C₉), 118.97 (phenyl-C₂₃), 116.05 (pyrrole-C₂, C₅), 113.47 (phenyl-C₂₅), 111.23 (pyrrole-C₃, C₄), 67.11 (-CH₂).

Mass (ESI- m/z) = Found 352.1259 [M^+ + H]; Calcd. 351.36).

CHN Anal. For C₁₉H₁₇N₃O₄: Calcd. C, 64.95; H, 4.88; N, 11.96; Found: C, 64.90; H, 4.79; N, 11.87.

3.3.4. Synthesis of (3d): N²-(2-(2,4-dimethylphenoxy)acetyl)-4-(1H-pyrrol-1-yl)benzohydrazide. White amorphous solid. (Yield 59%). M.p 190–192°C; FTIR (KBr-cm⁻¹): 3391 (NH), 3207 (NH), 2922 (Ar-C = CH), 1694 (C = O), 1613 (C = O).

^1H NMR (8 mg-DMSO- d_6 , 400 MHz, T-18.85°C, δ ppm): 10.49 (1H, s, CONH), 10.14 (1H, s, NHCO), 8.02 (2H, d, $J = 8.72$ Hz, bridging phenyl-C₈, C₁₀-H), 7.76 (2H, d, $J = 8.76$ Hz, bridging phenyl-C₇, C₁₁-H), 7.51 (2H, d, $J = 2.2$ Hz, pyrrole-C₂, C₅-H), 7.04 (2H, d, $J = 9.08$ Hz, phenyl-C₂₂, C₂₄-H), 6.86 (1H, d, $J = 2.2$ Hz, phenyl-C₂₅-H), 6.33–6.32 (2H, t, $J = 2.16$ Hz, $J = 2.12$ Hz, pyrrole-C₃, C₄-H), 4.65 (2H, s, CH₂-H), 2.22 (6H, s, di-CH₃-H).

^{13}C NMR (10 mg-DMSO- d_6 , 400 MHz, T-18.85°C, δ ppm): 167.44 (-NHCO), 164.61 (-CONH), 153.89 (phenyl-C₂₀), 142.27 (bridging phenyl-C₆), 131.24 (phenyl-C₂₃), 129.63 (bridging phenyl-C₈, C₁₀), 129.14 (bridging phenyl-C₇, C₁₁), 128.54 (phenyl-C₂₂, C₂₄), 126.95 (phenyl-C₂₁), 125.96 (bridging phenyl-C₉), 118.96 (pyrrole-C₂, C₅), 118.42 (phenyl-C₂₅), 111.69 (pyrrole-C₃, C₄), 66.58 (CH₂), 20.04 (phenyl-CH₃), 16.05 (phenyl-CH₃).

Mass (ESI- m/z) = Found 365.2626 [M^+ + 2]; Calcd. 363.42.

CHN Anal. For C₂₁H₂₁N₃O₃: Calcd. C, 69.41; H, 5.82; N, 11.56; Found: C, 69.39; H, 5.76; N, 11.54.

3.3.5. Synthesis of (3e): 4-(1H-pyrrol-1-yl)-N²-(2-(*m*-tolylloxy)acetyl)benzohydrazide. White amorphous solid. (Yield 77%). M.p 176–178°C; FTIR (KBr-cm⁻¹): 3357 (NH), 3236 (NH), 2922 (Ar-C = CH), 1694 (C = O), 1650 (C = O).

^1H NMR (8 mg-DMSO- d_6 , 400 MHz, T-18.85°C, δ ppm): 10.47 (1H, s, CONH), 10.25 (1H, s, NHCO), 8.01 (2H, d, $J = 8.60$ Hz, bridging phenyl-C₈, C₁₀-H), 7.78 (2H, d, $J = 8.44$ Hz, bridging phenyl-C₇, C₁₁-H), 7.52 (1H, d, $J = 1.72$ Hz, phenyl-C₂₅-H), 7.20 (2H, d, $J = 2.48$ Hz, pyrrole-C₂, C₅-H), 6.88–6.74 (3H, m, phenyl-C₂₁, C₂₂, C₂₃-H), 6.33 (2H, d, $J = 1.72$ Hz, pyrrole-C₃, C₄-H), 4.75 (2H, s, CH₂-H), 2.28 (3H, s, CH₃-H).

^{13}C NMR (10 mg-DMSO- d_6 , 400 MHz, T-18.85°C, δ ppm): 167.26 (-NHCO), 164.67 (-CONH), 157.74 (phenyl-C₂₀), 141.91 (bridging phenyl-C₆), 129.61 (bridging phenyl-C₈, C₁₀), 128.55 (bridging phenyl-C₇, C₁₁), 123.03 (phenyl-C₂₂, C₂₄), 121.96 (bridging phenyl-C₉), 121.09 (C-23), 115.36 (pyrrole-C₂, C₅), 111.77 (phenyl-C₂₁, C₂₅), 110.57 (pyrrole-C₃, C₄), 66.04 (CH₂), 21.09 (phenyl-CH₃).

Mass (ESI- m/z) = Found 349.2064 [M^+]; Calcd. 349.39.

CHN Anal. For C₂₀H₁₉N₃O₃: Calcd. C, 68.75; H, 5.48; N, 12.03; Found: C, 68.67; H, 5.46; N, 12.04.

3.3.6. Synthesis of (3f): N²-(2-(4-chlorophenoxy)acetyl)-4-(1H-pyrrol-1-yl)benzohydrazide. White amorphous solid. (Yield 68%). M.p 161–163°C; FTIR (KBr-cm⁻¹): 3373 (NH), 3257 (NH), 2915 (Ar-C = CH), 1723 (C = O), 1649 (C = O).

^1H NMR (8 mg-DMSO- d_6 , 400 MHz, T-18.85°C, δ ppm): 10.43 (1H, s, CONH), 10.26 (1H, s, NHCO), 8.00 (2H, d, J = 8.00 Hz, bridging phenyl-C₈, C₁₀-H), 7.75 (2H, d, J = 5.12 Hz, bridging phenyl-C₇, C₁₁-H), 7.48 (2H, d, J = 4.28 Hz, phenyl-C₂₂, C₂₄-H), 7.29 (2H, d, J = 5.16 Hz, pyrrole-C₂, C₅-H), 7.00–6.96 (3H, m, phenyl-C₂₁, C₂₁, C₂₅-H) 6.34 (2H, s, pyrrole-C₃, C₄-H), 4.65 (2H, s, CH₂-H).

^{13}C NMR (10 mg-DMSO- d_6 , 400 MHz, T-18.85°C, δ ppm): 166.90 (-NHCO), 164.58 (-CONH), 156.58 (phenyl-C₂₀), 143.89 (bridging phenyl-C₆), 130.90 (phenyl-C₂₂, C₂₄), 129.20 (bridging phenyl-C₈, C₁₀), 128.19 (phenyl-C₂₁, C₂₅), 124.98 (bridging phenyl-C₇, C₁₁), 122.97 (bridging phenyl-C₉), 121.03 (phenyl-C₂₂), 116.57 (pyrrole-C₂, C₅), 110.25 (pyrrole-C₃, C₄), 66.35 (CH₂).

Mass (ESI- m/z) = Found 371.0744 [M^+ + 2]; Calcd. 369.81.

CHN Anal. For C₁₉H₁₆ClN₃O₃: Calcd. C, 61.71; H, 4.36; N, 11.36; Found: C, 61.69; H, 4.32; N, 11.30.

3.3.7. Synthesis of (3g): N²-(2-(3,5-dihydroxyphenoxy)acetyl)-4-(1H-pyrrol-1-yl) benzohydrazide. White amorphous solid. (Yield 69%). M.p 160–162°C; FTIR (KBr-cm⁻¹): 3367 (NH), 3220 (NH), 2923 (Ar-C = CH), 1702 (C = O), 1621 (C = O).

^1H NMR (8 mg-DMSO- d_6 , 400 MHz, T-19.95°C, δ ppm): 10.46 (1H, s, CONH), 10.22 (1H, s, NHCO), 9.46 (1H, s, OH), 8.99 (1H, s, OH), 7.96 (1H, s, phenyl-C₂₁-H), 7.90 (1H, s, phenyl-C₂₅-H), 7.75 (2H, d, J = 4.56 Hz, bridging phenyl-C₈, C₁₀-H), 7.68 (2H, d, J = 7.76 Hz, bridging phenyl-C₇, C₁₁-H), 7.47 (2H, d, J = 2.2 Hz, pyrrole-C₂, C₅-H), 6.31 (2H, d, J = 2.16 Hz, pyrrole-C₃, C₄-H), 5.68 (1H, s, phenyl-C₂₃-H), 4.51 (2H, s, CH₂-H).

^{13}C NMR (10 mg-DMSO- d_6 , 400 MHz, T-19.95°C, δ ppm): 167.09 (-NHCO), 164.45 (-CONH), 158.87 (phenyl-C₂₀), 157.64 (phenyl-C₂₂, C₂₄), 141.83 (bridging phenyl-C₆), 129.35 (bridging phenyl-C₈, C₁₀), 129.18 (CH, C-7, C-11), 126.64 (bridging phenyl-C₉), 118.93 (bridging phenyl-C₇, C₁₁), 111.14 (pyrrole-C₃, C₄), 110.22 (phenyl-C₂₃), 94.01 (phenyl-C₂₁, C₂₅), 66.35 (CH₂).

Mass (ESI- m/z) = found 368.0277 [M^+ + H]; Calcd. 367.36.

CHN Anal. For C₁₉H₁₇N₃O₅: Calcd. C, 62.12; H, 4.66; N, 11.44; Found: C, 62.09; H, 4.61; N, 11.42.

3.3.8. Synthesis of (3h):N²-(2-(3,5-dimethylphenoxy)acetyl)-4-(1H-pyrrol-1-yl) benzohydrazide. White amorphous solid. (Yield 72%). M.p 166–168°C; FTIR (KBr-cm⁻¹): 3400 (NH), 3264 (NH), 2918 (Ar-C = CH), 1720 (C = O), 1600 (C = O).

^1H NMR (8 mg-DMSO- d_6 , 400 MHz, T-19.15°C, δ ppm): 10.50 (1H, s, CONH), 10.26 (1H, s, NHCO), 8.03 (2H, d, J = 7.04 Hz, bridging phenyl-C₈, C₁₀-H), 7.76 (2H, d, J = 8.84 Hz, bridging phenyl-C₇, C₁₁-H), 7.51 (2H, d, J = 2.28 Hz, pyrrole-C₂, C₅-H), 6.67 (2H, s, phenyl-C₂₁, C₂₅-H), 6.62 (1H, s, phenyl-C₂₃-H), 6.33 (2H, d, J = 2.24 Hz, pyrrole-C₃, C₄-H), 4.64 (2H, s, CH₂-H), 2.23 (6H, s, di-CH₃-H).

^{13}C NMR (10 mg-DMSO- d_6 , 400 MHz, T-19.15°C, δ ppm): 167.37 (-NHCO), 164.71 (-CONH), 157.74 (phenyl-C₂₀), 142.27 (phenyl-C₂₂, C₂₄), 138.62 (bridging phenyl-C₆), 129.16 (bridging phenyl-C₈, C₁₀), 128.53 (bridging phenyl-C₇, C₁₁), 122.82 (bridging phenyl-C₉), 118.94 (pyrrole-C₂, C₅), 119.41 (pyrrole-C₃, C₄), 112.45 (phenyl-C₂₃), 111.21 (phenyl-C₂₁, C₂₅), 65.99 (CH₂), 21.03 (di-CH₃).

Mass (ESI- m/z) = Found 363.1623 [M^+]; Calcd. 363.42.

CHN Anal. For C₂₁H₂₁N₃O₃: Calcd. C, 69.41; H, 5.82; N, 11.56; Found: C, 69.40; H, 5.79; N, 11.52.

3.3.9. Synthesis of (3i): N²-(2-(3-hydroxyphenoxy)acetyl)-4-(1H-pyrrol-1-yl)benzohydrazide. White amorphous solid. (Yield 67%). M.p 173–175°C; FTIR (KBr-cm⁻¹): 3387 (NH), 3277 (NH), 2924 (Ar-C = CH), 1723 (C = O), 1603 (C = O).

^1H NMR (8 mg-DMSO- d_6 , 400 MHz, T-19.15°C, δ ppm): 10.52 (1H, s, CONH), 10.26 (1H, s, NHCO), 9.01 (1H, s, OH-H), 8.03 (2H, d, $J = 7.14$ Hz, bridging phenyl-C₈, C₁₀-H), 7.76 (2H, d, $J = 8.24$ Hz, bridging phenyl-C₇, C₁₁-H), 7.51 (2H, d, $J = 2.24$ Hz, pyrrole-C₂, C₅-H), 6.66–6.51 (4H, m, phenyl-C₂₁, C₂₃, C₂₄, C₂₅-H), 6.33 (2H, d, $J = 2.24$, pyrrole-C₃, C₄-H), 4.85 (2H, s, CH₂-H).

^{13}C NMR (10 mg-DMSO- d_6 , 400 MHz, T-19.15°C, δ ppm): 167.25 (-NHCO), 164.90 (-CONH), 157.74 (phenyl-C₂₀), 141.31 (bridging phenyl-C₆), 131.35 (phenyl-C₂₄), 130.11 (phenyl-C₂₂), 129.17 (bridging phenyl-C₇, C₁₁), 128.83 (bridging phenyl-C₈, C₁₀), 128.15 (bridging phenyl-C₉), 121.97 (pyrrole-C₂, C₅), 111.78 (pyrrole-C₃, C₄), 108.32 (phenyl-C₂₃), 106.66 (phenyl-C₂₅), 102.12 (phenyl-C₂₁), 66.3 (CH₂).

Mass (ESI- m/z) = Found 352.2195 [M^+ + H]; Calcd. 351.36.

CHN Anal. For C₁₉H₁₇N₃O₄: Calcd. C, 64.95; H, 4.88; N, 11.96; Found: C, 64.91; H, 4.81; N, 11.89.

3.3.10. Synthesis of (3j): N²-(2-(2-chlorophenoxy)acetyl)-4-(1H-pyrrol-1-yl)benzohydrazide. White amorphous solid. (Yield 65%). M.p 156–158°C; FTIR (KBr- cm^{-1}): 3355 (NH), 3269 (NH), 2917 (Ar-C = CH), 1714 (C = O), 1647 (C = O).

^1H NMR (8 mg-DMSO- d_6 , 400 MHz, T-18.85°C, δ ppm): 10.55 (1H, s, CONH), 10.28 (1H, s, NHCO), 7.99 (2H, d, $J = 4.28$ Hz, bridging phenyl-C₈, C₁₀-H), 7.76 (2H, d, $J = 5.64$ Hz, bridging phenyl-C₇, C₁₁-H), 7.49 (2H, d, $J = 5.16$ Hz, pyrrole-C₂, C₅-H), 7.45–6.97 (4H, m, phenyl-C₂₂, C₂₃, C₂₄, C₂₅-H), 6.32 (2H, d, $J = 2.16$ Hz, pyrrole-C₃, C₄-H), 4.83 (2H, s, CH₂-H).

^{13}C NMR (10 mg-DMSO- d_6 , 400 MHz, T-18.85°C, δ ppm): 166.74 (-NHCO), 164.64 (-CONH), 153.37 (phenyl-C₂₀), 142.30 (bridging phenyl-C₆), 130.04 (phenyl-C₂₂, C₂₄), 129.16 (C-8, bridging phenyl-C₈, C₁₀), 128.41 (phenyl-C₂₁), 128.19 (bridging phenyl-C₇, C₁₁), 122.22 (bridging phenyl-C₉), 121.49 (phenyl-C₂₃), 118.95 (pyrrole-C₂, C₅), 114.22 (phenyl-C₂₃), 111.21 (pyrrole-C₃, C₄), 66.59 (CH₂).

Mass (ESI- m/z) = Found 371.5759 [M^+ + 2]; Calcd. 369.81.

CHN Anal. For C₁₉H₁₆ClN₃O₃: Calcd. C, 61.71; H, 4.36; N, 11.36; Found: C, 61.70; H, 4.32; N, 11.32.

3.3.11. Synthesis of (5a): 4-(2,5-dimethyl-1H-pyrrol-1-yl)-N²-(2-phenoxyacetyl) benzohydrazide. Yellow crystalline solid. (Yield 70%). M.p 140–142°C. FTIR (KBr- cm^{-1}): 3411 (NH), 3227 (NH), 2923 (Ar-C = CH), 1696 (C = O), 1647 (C = O).

^1H NMR (8 mg-DMSO- d_6 , 400 MHz, T-19.75°C, δ ppm): 10.58 (1H, s, CONH), 10.35 (1H, s, NHCO), 8.05 (2H, d, $J = 8.48$ Hz, bridging phenyl-C₈, C₁₀-H), 7.43 (2H, d, $J = 8.44$ Hz, bridging phenyl-C₇, C₁₁-H), 7.36–7.29 (2H, m, phenyl-C₂₄, C₂₆-H), 7.06–6.93 (3H, m, phenyl-C₂₃, C₂₅, C₂₇-H), 5.86 (2H, d, $J = 4.88$ Hz, pyrrole-C₃, C₄-H), 4.69 (2H, s, CH₂-H), 2.01 (6H, s, diCH₃-H).

^{13}C NMR (10 mg-DMSO- d_6 , 400 MHz, T-19.75°C, δ ppm): 167.22 (-NHCO), 164.93 (-CONH), 157.67 (phenyl-C₂₂), 141.32 (bridging phenyl-C₆), 131.30 (phenyl-C₂₄, C₂₆), 129.47 (bridging phenyl-C₇, C₁₁), 128.51 (bridging phenyl-C₈, C₁₀), 127.96 (bridging phenyl-C₉), 121.26 (pyrrole-C₂, C₅), 114.71 (phenyl-C₂₅), 114.40 (CH, phenyl-C₂₃, C₂₇), 106.48 (CH, pyrrole-C₃, C₄), 66.05 (CH₂), 12.85 (pyrrole-diCH₃).

Mass (ESI- m/z) = Found 363.1381 [M^+]; Calcd. 363.42.

CHN Anal. For C₂₁H₂₁N₃O₃: Calcd. C, 69.41; H, 5.82; N, 11.56; Found: C, 69.40; H, 5.78; N, 11.55.

3.3.12. Synthesis of (5b): 4-(2,5-dimethyl-1H-pyrrol-1-yl)-N²-(2-(p-tolyloxy)acetyl) benzohydrazide. Yellow crystalline solid. (Yield 65%). M.p 164–166°C. FTIR (KBr- cm^{-1}): 3391 (NH), 3190 (NH), 2920 (Ar-C = CH), 1698 (C = O), 1653 (C = O).

^1H NMR (8 mg-DMSO- d_6 , 400 MHz, T-22.15°C, δ ppm): 10.54 (1H, s, CONH), 10.29 (1H, s, NHCO), 8.03 (2H, d, $J = 6.72$ Hz, bridging phenyl-C₈, C₁₀-H), 7.43 (2H, d, $J = 8.44$ Hz,

bridging phenyl-C₇, C₁₁-H), 7.14 (2H, d, *J* = 8.32 Hz, phenyl-C₂₄, C₂₆-H), 6.94 (2H, d, *J* = 8.56 Hz, phenyl-C₂₃, C₂₇-H), 5.84 (2H, s, pyrrole-C₃, C₄-H), 4.63 (2H, s, CH₂-H), 2.24 (3H, s, phenyl-CH₃-H), 2.03 (6H, s, pyrrole-diCH₃-H).

¹³C NMR (10 mg-DMSO-d₆, 400 MHz, T-22.15°C, δ ppm): 167.29 (-NHCO), 164.89 (-CONH), 155.63 (phenyl-C₂₂), 141.30 (bridging phenyl-C₆), 131.32 (phenyl-C₂₄, C₂₆), 129.99 (bridging phenyl-C₇, C₁₁), 129.78 (bridging phenyl-C₈, C₁₀), 128.49 (bridging phenyl-C₉), 127.51 (pyrrole-C₂, C₅), 114.58 (phenyl-C₂₅), 112.14 (phenyl-C₂₃, C₂₇), 106.47 (pyrrole-C₃, C₄), 66.2 (CH₂), 12.85 (phenyl-C₂₅), 20.05 (phenyl-diCH₃), 12.85 (pyrrole-diCH₃).

Mass (ESI- *m/z*) = Found 377.1119 [M⁺]; Calcd. 377.44.

CHN Anal. For C₂₂H₂₃N₃O₃: Calcd. C, 70.01; H, 6.14; N, 11.13; Found: C, 70.01; H, 6.14; N, 11.13.

3.3.13. Synthesis of (5c) 4-(2,5-dimethyl-1H-pyrrol-1-yl)-N'-(2-(2-hydroxyphenoxy) acetyl) benzohydrazide. Yellow crystalline solid. (Yield 60%). M.p 180–182°C. FTIR (KBr-cm⁻¹): 3403 (OH), 3312 (NH), 3273 (NH), 2922 (Ar-C = CH), 1651 (C = O), (C = O).

¹H NMR (8 mg-DMSO-d₆, 400 MHz, T-21.85°C, δ ppm): 10.61 (1H, s, CONH), 10.33 (1H, s, NHCO), 8.99 (1H, s, OH), 8.03 (2H, d, *J* = 8.76 Hz, bridging phenyl-C₈, C₁₀-H), 7.52 (2H, d, *J* = 6.24 Hz, bridging phenyl-C₇, C₁₁-H), 7.04–6.85 (4H, m, phenyl-C₂₄, C₂₅, C₂₆, C₂₇-H), 6.31 (2H, s, pyrrole-C₃, C₄), 4.78 (2H, s, CH₂-H), 1.84 (6H, s, pyrrole-diCH₃-H).

¹³C NMR (10 mg-DMSO-d₆, 400 MHz, T-21.85°C, δ ppm): 167.06 (-NHCO), 165.13 (-CONH), 146.10 (phenyl-C₂₂), 145.26 (bridging phenyl-C₆), 128.52 (phenyl-C₂₄), 128.01 (bridging phenyl-C₇, C₁₁), 127.53 (CH, bridging phenyl-C₈, C₁₀), 122.19 (bridging phenyl-C₉), 119.36 (pyrrole-C₂, C₅), 116.08 (phenyl-C₂₅, C₂₆), 113.43 (phenyl-C₂₃, C₂₇), 106.50 (pyrrole-C₃, C₄), 67.06 (CH₂), 12.82 (pyrrole-diCH₃).

Mass (ESI- *m/z*) = Found 380.1251 [M⁺ + H]; Calcd. 379.42.

CHN Anal. For C₂₁H₂₁N₃O₄: Calcd. C, 66.48; H, 5.58; N, 11.08; Found: C, 66.48; H, 5.58; N, 11.08.

3.3.14. Synthesis of (5d): 4-(2,5-dimethyl-1H-pyrrol-1-yl)-N'-(2-(2,4-dimethylphenoxy) acetyl) benzohydrazide. Yellow crystalline solid. (Yield 55%). M.p 186–188°C. FTIR (KBr-cm⁻¹): 3350 (NH), 3226 (NH), 2921 (Ar-C = CH), 1700 (C = O), 1653 (C = O).

¹H NMR (8 mg-DMSO-d₆, 400 MHz, T-22.15°C, δ ppm): 10.57 (1H, s, CONH), 10.20 (1H, s, NHCO), 8.04 (2H, d, *J* = 8.46 Hz, bridging phenyl-C₈, C₁₀-H), 7.42 (2H, d, *J* = 8.52 Hz, bridging phenyl-C₇, C₁₁-H), 6.98–6.84 (3H, m, phenyl-C₂₄, C₂₆, C₂₇-H), 5.84 (2H, s, pyrrole-C₃, C₄), 4.65 (2H, s, phenyl-C₂₀-H), 2.22 (3H, s, phenyl-C₂₉-CH₃-H), 2.18 (3H, s, phenyl-C₂₈-CH₃-H), 1.99 (6H, s, pyrrole-diCH₃-H).

¹³C NMR (10 mg-DMSO-d₆, 400 MHz, T-22.15°C, δ ppm): 167.46 (-NHCO), 164.84 (CONH), 153.89 (phenyl-C₂₄), 141.30 (bridging phenyl-C₆), 131.32 (phenyl-C₂₆), 129.66 (bridging phenyl-C₇, C₁₁), 128.50 (bridging phenyl-C₈, C₁₀), 127.95 (bridging phenyl-C₉), 126.95 (phenyl-C₂₂), 125.97 (pyrrole-C₂, C₅), 114.71 (phenyl-C₂₅), 111.71 (phenyl-C₂₃, C₂₇), 106.47 (pyrrole-C₃, C₄), 66.58 (CH₂), 20.03 (phenyl-C₂₈-CH₃), 16.05 (phenyl-C₂₉-CH₃-H), 12.85 (pyrrole-diCH₃-H).

Mass (ESI- *m/z*) = Found 391.2626 [M⁺]; Calcd. 391.19.

CHN Anal. For C₂₃H₂₅N₃O₃: Calcd. C, 70.57; H, 6.44; N, 10.73; Found: C, 70.57; H, 6.44; N, 10.73.

3.3.15. Synthesis of (5e): 4-(2,5-dimethyl-1H-pyrrol-1-yl)-N'-(2-(*m*-tolylloxy) acetyl) benzohydrazide. Yellow crystalline solid. (Yield 67%). M.p 170–172°C; FTIR (KBr-cm⁻¹): 3378 (NH), 3223 (NH), 2921 (Ar-C = CH), 1697 (C = O), 1649 (C = O).

¹H NMR (8 mg-DMSO-d₆, 400 MHz, T-22.45°C, δ ppm): 10.57 (1H, s, CONH), 10.32 (1H, s, NHCO), 8.11 (2H, d, *J* = 8.48 Hz, bridging phenyl-C₈, C₁₀-H), 7.45 (2H, d, *J* = 8.52 Hz, bridging phenyl-C₇, C₁₁-H), 7.22–6.74 (4H, m, phenyl-C₂₄, C₂₅, C₂₆, C₂₇-H), 5.84 (2H, s,

pyrrole-C₃, C₄), 4.67 (2H, s, CH₂-H), 2.31 (3H, s, phenyl-C₂₈.CH₃.H), 2.02 (6H, s, pyrrole-diCH₃.H).

¹³C NMR (10 mg-DMSO-d₆, 400 MHz, T-22.45°C, δ ppm): 167.25 (NHCO), 164.90 (CONH), 157.74 (phenyl-C₂₂), 141.31 (bridging phenyl-C₆), 138.98 (phenyl-C₂₄, C₋₂₆), 131.35 (bridging phenyl-C₇, C₁₁), 130.11 (bridging phenyl-C₈, C₁₀), 129.17 (bridging phenyl-C₉), 121.97 (pyrrole-C₂, C₅), 115.36 (phenyl-C₂₅), 111.78 (phenyl-C₂₃, C₂₇), 106.66 (pyrrole-C₃, C₄), 66.05 (CH₂), 21.07 (phenyl-C₂₈ -CH₃), 12.85 (pyrrole-diCH₃.H).

Mass (ESI- *m/z*) = Found 377.4952 [M⁺]; Calcd. 377.44.

CHN Anal. For C₂₂H₂₃N₃O₃: Calcd. C, 70.01; H, 6.14; N, 11.13; Found: C, 70.01; H, 6.14; N, 11.13.

3.3.16. Synthesis of (5f): N²-(2-(4-chlorophenoxy)acetyl)-4-(2,5-dimethyl-1H-pyrrol-1-yl) benzohydrazide. Yellow crystalline solid. (Yield 78%). M.p 156–158°C. FTIR (KBr-cm⁻¹): 3385 (NH), 3248 (NH), 2922 (Ar-C = CH), 1681 (C = O), 1647 (C = O).

¹H NMR (8 mg-DMSO-d₆, 400 MHz, T-25.51°C, δ ppm): 10.55 (1H, s, CONH), 10.33 (1H, s, NHCO), 8.03 (2H, d, *J* = 8.48 Hz, bridging phenyl-C₈, C₁₀-H), 7.43 (2H, d, *J* = 8.92 Hz, bridging phenyl-C₇, C₁₁-H), 7.40 (2H, d, *J* = 5.52 Hz, phenyl-C₂₄, C₂₆-H), 7.08 (2H, d, *J* = 6.76 Hz, phenyl-C₂₃, C₂₇-H), 5.84 (2H, s, pyrrole-C₃, C₄), 4.70 (2H, s, CH₂-H), 2.00 (6H, s, pyrrole-diCH₃.H).

¹³C NMR (10 mg-DMSO-d₆, 400 MHz, T-25.51°C, δ ppm): 166.90 (NHCO), 164.92 (CONH), 157.57 (phenyl-C₂₂), 141.32 (bridging phenyl-C₆), 131.30 (phenyl-C₂₄, C₋₂₆), 129.20 (bridging phenyl-C₇, C₁₁), 128.50 (bridging phenyl-C₈, C₁₀), 127.97 (bridging phenyl-C₉), 127.51 (pyrrole-C₂, C₅), 125.01 (phenyl-C₂₅), 116.52 (phenyl-C₂₃, C₂₇), 106.48 (pyrrole-C₃, C₄), 66.35 (CH₂), 12.84 (pyrrole-diCH₃.H).

Mass (ESI- *m/z*) = Found 399.7788 [M⁺ + 2]; Calcd. 397.86.

CHN Anal. For C₁₉H₁₆ClN₃O₃: Calcd. C, 63.40; H, 5.07; Cl, 8.91; N, 10.56; Found: C, 63.40; H, 5.07; Cl, 8.91; N, 10.56.

3.3.17. Synthesis of (5g): N²-(2-(3,5-dihydroxyphenoxy)acetyl)-4-(2,5-dimethyl-1H-pyrrol-1-yl) benzohydrazide. Yellow crystalline solid. (Yield 88%). M.p 160–162°C; FTIR (KBr-cm⁻¹): 3355 (NH), 3224 (NH), 2923 (Ar-C = CH), 1711 (C = O), 1643 (C = O).

¹H NMR (8 mg-DMSO-d₆, 500 MHz, T-26.05°C, δ ppm): 10.30 (1H, s, CONH), 10.20 (1H, s, NHCO), 8.97 (2H, s, OH), 8.07 (2H, d, *J* = 8.80 Hz, bridging phenyl-C₈, C₁₀-H), 7.98 (2H, d, *J* = 7.66 Hz, bridging phenyl-C₇, C₁₁-H), 7.48 (2H, d, *J* = 8.5 Hz, phenyl-C₂₃, C₂₇-H), 7.01 (1H, s, phenyl-C₂₅-H), 5.93 (2H, s, pyrrole-C₃, C₄), 4.34 (2H, s, CH₂-H), 1.99 (6H, s, pyrrole-diCH₃.H).

¹³C NMR (10 mg-DMSO-d₆, 500 MHz, T-26.65°C, δ ppm): 166.21 (NHCO), 165.10 (CONH), 159.02 (phenyl-C₂₂), 158.11 (bridging phenyl-C₆), 140.40 (phenyl-C₂₄), 130.59 (phenyl-C₂₆), 129.26 (bridging phenyl-C₇, C₁₁), 128.61 (bridging phenyl-C₈, C₁₀), 127.99 (bridging phenyl-C₉), 126.54 (pyrrole-C₂, C₅), 123.78 (phenyl-C₂₅), 107.15 (phenyl-C₂₃, C₂₇), 100.72 (pyrrole-C₃, C₄), 61.38 (CH₂), 13.28 (pyrrole-diCH₃.H).

Mass (ESI- *m/z*) = Found 396.2720 [M⁺ + H]; Calcd. 395.42.

CHN Anal. For C₂₁H₂₁N₃O₅: Calcd. C, 63.79; H, 5.35; N, 10.63; Found: C, 63.79; H, 5.35; N, 10.63.

3.3.18. Synthesis of (5h): 4-(2,5-dimethyl-1H-pyrrol-1-yl)-N²-(2-(3,5-dimethylphenoxy)acetyl) benzohydrazide. Yellow solid. (Yield 76%). M.p 158–160°C. FTIR (KBr-cm⁻¹): 3318 (NH), 3235 (NH), 2920 (Ar-C = CH), 1649 (C = O), 1604 (C = O).

¹H NMR (8 mg-DMSO-d₆, 500 MHz, T-26.05°C, δ ppm): 10.55 (1H, s, CONH), 10.28 (1H, s, NHCO), 8.05 (2H, d, *J* = 8.50 Hz, bridging phenyl-C₈, C₁₀-H), 7.44 (2H, d, *J* = 7.55 Hz, bridging phenyl-C₇, C₁₁-H), 6.61 (2H, d, *J* = 8.5 Hz, phenyl-C₂₃, C₂₇-H), 6.58 (1H, s, phenyl-

C₂₅-H), 5.86 (2H, d, *J* = 4.80 Hz, pyrrole-C₃, C₄), 4.64 (2H, s, CH₂-H), 2.26 (6H, s, phenyl-diCH₃-H), 1.99 (6H, s, pyrrole-diCH₃-H).

¹³C NMR (10 mg-DMSO-d₆, 500 MHz, T-26.65°C, δ ppm): 167.80 (NHCO), 165.77 (CONH), 155.28 (phenyl-C₂₂), 148.01 (bridging phenyl-C₆), 141.81 (phenyl-C₂₄), 130.61 (phenyl-C₂₆), 129.61 (bridging phenyl-C₇, C₁₁), 128.66 (bridging phenyl-C₈, C₁₀), 127.11 (bridging phenyl-C₉), 126.54 (pyrrole-C₂, C₅), 123.30 (phenyl-C₂₅), 112.65 (phenyl-C₂₃, C₂₇), 106.97 (pyrrole-C₃, C₄), 66.55 (CH₂), 15.07 (phenyl-diCH₃-H), 14.61 (pyrrole-diCH₃-H).

Mass (ESI- *m/z*) = Found 391.7207 [M⁺]; Calcd. 391.47.

CHN Anal. For C₂₃H₂₅N₃O₃: Calcd. C, 70.57; H, 6.44; N, 10.73; Found: C, 70.57; H, 6.44; N, 10.73.

3.3.19. Synthesis of (5i): 4-(2,5-dimethyl-1H-pyrrol-1-yl)-N'-(2-(3-hydroxyphenoxy)acetyl) benzohydrazide. Yellow crystalline solid. (Yield 70%). M.p 124–126°C; FTIR (KBr-cm⁻¹): 3433 (OH), 3321 (NH), 3278 (NH), 2922 (Ar-C = CH), 1697 (C = O), 1652 (C = O).

¹H NMR (8 mg-DMSO-d₆, 500 MHz, T-26.05°C, δ ppm): 10.59 (1H, s, CONH), 10.29 (1H, s, NHCO), 9.50 (1H, s, OH), 8.07 (2H, d, *J* = 8.50 Hz, bridging phenyl-C₈, C₁₀-H), 7.42 (2H, d, *J* = 8.50 Hz, bridging phenyl-C₇, C₁₁-H), 7.11–6.92 (4H, m, phenyl-C₂₃, C₂₅, C₂₆, C₂₇-H), 5.87 (2H, d, *J* = 5.28 Hz, pyrrole-C₃, C₄), 4.62 (2H, s, CH₂-H), 2.03 (6H, s, pyrrole-diCH₃-H).

¹³C NMR (10 mg-DMSO-d₆, 500 MHz, T-26.65°C, δ ppm): 167.68 (NHCO), 165.38 (CONH), 159.02 (phenyl-C₂₂), 158.82 (phenyl-C₂₄), 151.29 (bridging phenyl-C₆), 141.83 (phenyl-C₂₆), 130.61 (bridging phenyl-C₇, C₁₁), 128.68 (bridging phenyl-C₈, C₁₀), 113.68 (bridging phenyl-C₉), 112.39 (pyrrole-C₂, C₅), 109.28 (phenyl-C₂₅), 107.18 (phenyl-C₂₃), 106.70 (phenyl-C₂₇), 102.40 (pyrrole-C₃, C₄), 66.59 (CH₂), 13.34 (pyrrole-diCH₃-H).

Mass (ESI- *m/z*) = Found 381.2321 [M⁺+H]; Calcd. 379.42.

CHN Anal. For C₂₁H₂₁N₃O₄: Calcd. C, 66.48; H, 5.58; N, 11.08; Found: C, 66.48; H, 5.58; N, 11.08.

3.3.20. Synthesis of (5j): N'-(2-(2-chlorophenoxy)acetyl)-4-(2,5-dimethyl-1H-pyrrol-1-yl) benzohydrazide. Yellow crystalline solid. (Yield 55%). M.p 172–174°C. FTIR (KBr-cm⁻¹): 3390 (NH), 3243 (NH), 2928 (Ar-C = CH), 1679 (C = O), 1648 (C = O).

¹H NMR (8 mg-DMSO-d₆, 500 MHz, T-26.05°C, δ ppm): 10.41 (1H, s, CONH), 10.23 (1H, s, NHCO), 8.07 (2H, d, *J* = 8.28 Hz, bridging phenyl-C₈, C₁₀-H), 7.42 (2H, d, *J* = 8.22 Hz, bridging phenyl-C₇, C₁₁-H), 7.30–7.28 (2H, m, phenyl-C₂₄, C₂₆-H), 7.04–6.98 (2H, m, phenyl-C₂₅, C₂₇-H), 5.84 (2H, s, pyrrole-C₃, C₄), 4.66 (2H, s, CH₂-H), 2.04 (6H, s, pyrrole-diCH₃-H).

¹³C NMR (10 mg-DMSO-d₆, 500 MHz, T-26.65°C, δ ppm): 166.41 (NHCO), 165.92 (CONH), 156.18 (phenyl-C₂₂), 144.40 (phenyl-C₂₅), 141.34 (bridging phenyl-C₆), 132.16 (phenyl-C₂₄, C₂₆), 129.44 (bridging phenyl-C₇, C₁₁), 128.20 (bridging phenyl-C₈, C₁₀), 127.83 (bridging phenyl-C₉), 122.36 (pyrrole-C₂, C₅), 118.71 (phenyl-C₂₃), 116.26 (phenyl-C₂₇), 106.48 (pyrrole-C₃, C₄), 66.65 (CH₂), 12.95 (pyrrole-diCH₃-H).

Mass (ESI- *m/z*) = Found 399.6951 [M⁺+2]; Calcd. 397.86).

CHN Anal. For C₂₁H₂₀ClN₃O₃: Calcd. C, 63.40; H, 5.07; Cl, 8.91; N, 10.56; Found: C, 63.40; H, 5.07; Cl, 8.91; N, 10.56;

3.4. Molecular docking using Surflex-Dock

The study employed the patented Sybyl-X 2.0 search tool and Surflex-Dock for molecular docking analysis. The aim of this study was to provide a comprehensive understanding of the molecular interactions between chemicals and the active sites of the ENR enzyme and DHFR enzyme [30]. This work provides a thorough analysis that can be applied to enhance the future optimization of molecular architectures. The crystallographic structures of enoyl acyl carrier protein reductase InhA, in complex with N-(4-methylbenzoyl)-4-benzylpiperidine (PDB ID

2NSD, resolution of 1.9 Å by X-ray diffraction), and dihydrofolate reductase of *Mycobacterium tuberculosis*, bound to NADPH and methotrexate, were obtained from the Brookhaven Protein Database (PDB) located at <http://www.rcsb.org/pdb>. The ligands and protein employed in our docking methods were produced using the known Sybyl-X 2.0 standard protocol [31,32]. The inclusion of hydrogen atoms was necessary in order to establish the accurate configuration and tautomeric states. Subsequently, the structural model underwent energy minimization via the Tripos force field, incorporating a distance-dependent dielectric function. Partial atomic charges were then computed using the AM-BER7F9902 method. Lastly, the model was purged of water molecules. The molecular geometry of CP was later refined to achieve minimal energy by the utilization of the Powell energy minimization method. This process involved employing the Tripos force field together with Gasteiger-Hückel charges. Subsequently, the CP molecule was individually inserted into the binding pocket to facilitate the investigation of docking and scoring. In order to ascertain the interactions between the ligand and protein, the highest-ranking posture and protein were imported into the working environment. The MOLCAD application, which is a tool for molecular computer-aided design, was utilized to depict the manner in which the protein and ligand bind together.

3.5. ADMET studies

The toxicities were predicted using ProTox-II, and the corresponding results are shown in [Table 5](#). Additionally, the Molecular ADME properties were estimated using the in silico Swiss ADME online tool [33–36], and the results are presented in [Table 4](#).

3.6. MTT-based cytotoxicity activity

The cytotoxic activity (IC_{50}) of selected compounds against A549 (lung adenocarcinoma) MV cell-lines was evaluated by performing cellular conversion of MTT [3-(4,5-dimethylthiazol-2-yl)-2,5-diphenyl-tetrazolium bromide] into a formazan product. This evaluation was conducted up to a concentration of 50 mg/mL using the Promega Cell Titer 96 non-radioactive cell proliferation assay, with cisplatin serving as the positive control. Cytotoxicity is commonly quantified by determining the IC_{50} value, which represents the quantity of a substance that reduces the optical density of treated cells by 50% compared to untreated cells, as measured by the MTT experiment. The IC_{50} values presented in [Table 6](#) are the mean values \pm standard error of the mean (SEM) obtained from three separate and independent measurements.

3.6. Antitubercular activity

The efficacy of the newly synthesized compounds was assessed against the *M. tuberculosis* strain H37Rv using the Microplate Alamar Blue test (MABA). The obtained data, including the minimum inhibitory concentration (MIC) values, are presented in [Table 3](#) [37].

3.7. Antibacterial activity

The antibacterial inhibitory effects of all compounds were assessed using the broth microdilution method, with ciprofloxacin serving as the reference medication. The study focused on comparing the inhibitory effects against *S. aureus* (Gram-positive) and *E. coli* (Gram-negative) bacteria [38,39]. The antibacterial activity data, including the minimum inhibitory concentration (MIC) values, was summarized in [Table 3](#).

Table 6. Shows the *in vitro* cytotoxicity activity of selected drugs against human lung cancer (A549) cell lines, and MV cell lines (IC₅₀ in µg/mL).

| Compound | IC ₅₀ (µM) ^a | |
|----------|------------------------------------|-------------------|
| | MV cell-lines ^b | A549 ^c |
| 3a | - | - |
| 3b | - | - |
| 3c | 223±0.7 | 224±0.6 |
| 3d | 216±0.4 | 212±0.4 |
| 3e | - | - |
| 3f | | |
| 3g | 216±0.5 | 216±0.5 |
| 3h | 219±0.6 | 219±0.1 |
| 3i | | |
| 3j | | |
| 5a | | |
| 5b | - | - |
| 5c | - | - |
| 5d | 226±0.5 | 222±0.5 |
| 5e | 220±0.2 | 219±0.3 |
| 5f | | |
| 5g | | |
| 5h | | |
| 5i | | |
| 5j | | |
| INH | >450 | >450 |

^a Values are the means ± SEM of three independent experiments.

^b Mammalian Vero cell-lines (NCCS-Pune, INDIA).

^c A549 (lung adenocarcinoma) cell-lines (NCCS-Pune, INDIA).

<https://doi.org/10.1371/journal.pone.0303173.t006>

4. Conclusion

The antitubercular and enzyme inhibitory effects of a set of 20 newly synthesized pyrrolyl-benzohydrazide derivatives were assessed. All the compounds had moderate to good potency against tuberculosis, as shown by MICs ranging from 1.6 to 12.5 µg/ml. The derivatives were subjected to molecular docking analysis, revealing that these newly identified inhibitors exhibited a close match inside the binding site of both the ENR-enzyme and DHFR enzyme, similar to the 2NSD_ligand and 1DF7_ligand. *In vitro* assays indicated that the compounds **3c**, **3d**, **3g**, **3h**, **5a**, **5d** and **5e**, have significant enzyme inhibitory action (against both enzymes). It is therefore proposed that chemical scaffolds have generated novel single molecules that exert antitubercular activity, at least partly through targeting DHFR and ENR-enzymes. We anticipate that the analogues disclosed in this work will aid global efforts to identify prospective lead compounds for further development of the novel entities with dual DHFR and ENR-enzyme inhibitory properties.

5. Future implications

There are several important steps to consider for advancing the development of dual inhibitors in tuberculosis treatment. These steps may involve *in vivo* studies to evaluate pharmacokinetics, efficacy, and safety; enhancing compound properties to improve potency and selectivity;

exploring new biological targets for dual inhibition; addressing drug resistance and developing countermeasures; assessing toxicity and safety profiles; studying the pharmacodynamics and pharmacokinetics of dual inhibitors; and performing preclinical efficacy studies in appropriate animal models. These research directions aim to advance the development of effective and safe dual inhibitors, addressing drug resistance and improving treatment outcomes for tuberculosis.

Supporting information

S1 Graphical abstract.

(TIF)

S1 File. The supplementary files contains the spectral data for different synthesized compounds.

(DOC)

Acknowledgments

The authors are thankful to Dr. H. V. Dambal, President, and Dr. V. G. Jamakandi, Professor and Dean, Dr. V. H. Kulkarni, Principal, of SET's College of Pharmacy in Dharwad, Karnataka, India. For the NMR and mass spectral data, we also acknowledge SAIF, Panjab University in Chandigarh, Punjab, and IIT-Kanpur in India.

Author Contributions

Conceptualization: Sravanthi Avunoori, Ahmed Saif, Prem Kumar S. R., Shrinivas D. Joshi.

Data curation: Mater H. Mahnashi, Farkad Bantun, Abdulrahman Ali Alhadi.

Formal analysis: Sanjay Gopi, Hani Saleh Faidah, Abdulrahman Ali Alhadi, Jaber Hassan Alshehri.

Funding acquisition: Ibrahim Ahmed Shaikh, Abdullah Ali Alharbi.

Investigation: Sravanthi Avunoori, Sanjay Gopi, Shrinivas D. Joshi.

Methodology: Sravanthi Avunoori, Hani Saleh Faidah.

Project administration: Prem Kumar S. R., Shrinivas D. Joshi.

Resources: Ibrahim Ahmed Shaikh, Ahmed Saif, Jaber Hassan Alshehri, Abdullah Ali Alharbi.

Software: Farkad Bantun.

Visualization: Ibrahim Ahmed Shaikh.

Writing – original draft: Sravanthi Avunoori, Shrinivas D. Joshi.

Writing – review & editing: Mater H. Mahnashi, Sanjay Gopi, Ibrahim Ahmed Shaikh, Ahmed Saif, Farkad Bantun, Hani Saleh Faidah, Abdulrahman Ali Alhadi, Jaber Hassan Alshehri, Abdullah Ali Alharbi, Prem Kumar S. R.

References

1. Daniel T.M. The history of tuberculosis. *Respir Med.*, 2006, 100, 1862–1870.
2. World Health Organization, Tuberculosis. https://www.who.int/health-topics/tuberculosis#tab=tab_1. (Accessed 17 May 2021)
3. Diacon A.H.; Donald P.R.; Pym A.; Grobusch M.; Patientia R.F.; Mahanyele R.; Bantubani N.; Narasimooloo R.; De Marez T.; Van Heeswijk R.; Lounis N. Randomized pilot trial of eight weeks of

- bedaquiline (TMC207) treatment for multidrug-resistant tuberculosis: long-term outcome, tolerability, and effect on emergence of drug resistance, *Antimicrob. Agents Chemother.* 2012, 56, 3271–3276.
4. Mitnick C.D.; Shin S.S.; Seung K.J.; Rich M.L.; Atwood S.S.; Furin J.J.; Fitzmaurice G.M.; Alcantara Viru.; Appleton S.C.; Bayona J.N.; Bonilla C.A. Comprehensive treatment of extensively drug-resistant tuberculosis, *N. Engl. J. Med.* 2008, 359, 563–574. <https://doi.org/10.1056/NEJMoa0800106> PMID: 18687637
 5. Grobusch M.P. Drug-resistant and extensively drug-resistant tuberculosis in southern Africa, *Curr. Opin. Pulm. Med.* 2010, 16, 180–185. <https://doi.org/10.1097/MCP.0b013e3283378680> PMID: 20154624
 6. Matteelli A.; Migliori G.B.; Cirillo D.; Centis R.; Girard E.; Raviglione M. Multi drug resistant and extensively drug-resistant Mycobacterium tuberculosis: epidemiology and control, *Expert Rev. Anti. Infect. Ther.* 2007, 5, 857–871.
 7. Migliori G.B.; Richardson M.D.; Sotgiu G.; Lange C. Multidrug-resistant and extensively drug-resistant tuberculosis in the West, Europe and United States: epidemiology, surveillance, and control, *Clin. Chest. Med.* 2009, 30, 637–665.
 8. Datta B.S.; Hassan G.; Kadri S.M.; Qureshi W.; Kamili M.A.; Singh H.; Manzoor A.; Wani M.A.; Din S. U.; Thakur N. Multidrug-resistant and extensively drug resistant tuberculosis in Kashmir, India, *J. Infect. Dev. Ctries.* 2010, 4, 19–23. <https://doi.org/10.3855/jidc.669> PMID: 20130374
 9. Raviglione M.C.; Smith I.M. XDR tuberculosis implications for global public health, *N. Engl. J. Med.* 2007, 356, 656–659. <https://doi.org/10.1056/NEJMp068273> PMID: 17301295
 10. Rajasekaran S.; Chandrasekar C.; Mahilmaran A.; Kanakaraj K.; Karthikeyan D.S.; Suriakumar J. HIV coinfection among multidrug resistant and extensively drug resistant tuberculosis patients—A trend, *J. Indian Med. Assoc.* 2009, 107, 281–282. PMID: 19886382
 11. Myneedu V.P.; Visalakshi P.; Verma A.K.; Behera D.; Bhalla M. Prevalence of XDR TB cases—a retrospective study from a tertiary care TB hospital, *Indian J. Tuberc.* 2011, 58, 54–59. PMID: 21644390
 12. Tomioka H. Current status and perspective on drug targets in tubercle bacilli and drug design of antituberculous agents based on structure-activity relationship. *Curr Pharm Des.* 2014, 20, 4305–4306.
 13. Prem Kumar S.R.; Shaikh I.A.; Mahnashi M.H.; Alshahrani M.A.; Dixit S.R.; Kulkarni V.H.; Lherbet C.; Gadad A.K.; Aminabhavi T.M.; Joshi S.D. Design, synthesis and computational approach to study novel pyrrole scaffolds as active inhibitors of enoyl ACP reductase (InhA) and *Mycobacterium tuberculosis* antagonists. *J. Indian Chem. Soc.* 2022, 99, 100674. <https://doi.org/10.1016/j.jics.2022.100674>
 14. Dover L.G.; Bhatt A.; Bhowruth V.; Willcox B.E.; Besra G.S. New drugs and vaccines for drug-resistant Mycobacterium tuberculosis infections. *Expert Rev Vaccines.* 2008, 7, 481–497. <https://doi.org/10.1586/14760584.7.4.481> PMID: 18444894
 15. Azab I.H.E.; Elkanzi N.A.A. Synthesis and pharmacological evaluation of some new chromeno[3,4-c]pyrrole-3,4-dione-based N-heterocycles as antimicrobial agents. *J Heterocycl Chem.* 2017, 54, 1404–1414.
 16. Pegklidou K.; Papastavrou N.; Gkizis P.; Komiotis D.; Balzarini J.; Nicolaou I. N-substituted pyrrole-based scaffolds as potential anticancer and antiviral lead structures. *Med Chem.* 2015, 11, 602–608. <https://doi.org/10.2174/1573406411666150313161225> PMID: 25770917
 17. Yao J.; Takenaga K.; Koshikawa N.; Kida Y.; Lin J.; Watanabe T.; Maru Y.; Hippo Y.; Yamamoto S.; Zhu Y.; Nagase H. Anticancer effect of a pyrrole-imidazole polyamide-triphenylphosphonium conjugate selectively targeting a common mitochondrial DNA cancer risk variant in cervical cancer cells. *Int J Cancer.* 2023, 152, 962–976. <https://doi.org/10.1002/ijc.34319> PMID: 36214789
 18. Biava M.; Porretta G.C.; Poce G.; Supino S.; Deidda D.; Pompei R.; Molicotti P.; Manetti F.; Botta M. Antimycobacterial Agents. Novel Diarylpyrrole Derivatives of BM212 Endowed with High Activity toward Mycobacterium Tuberculosis and Low Cytotoxicity. *J. Med. Chem.* 2006, 49, 4946–4952. <https://doi.org/10.1021/jm0602662> PMID: 16884306
 19. Venugopala K.N.; Uppar V.; Chandrashekarappa S.; Abdallah H.H.; Pillay M.; Deb P.K.; Morsy M.A.; Aldhubiab B.E.; Attimarad M.; Nair A.B.; Sreeharsha N.; Tratratt C.; Yousef Jaber A.; Venugopala R.; Mailavaram R.P.; Al-Jaidi B.A.; Kandeel M.; Haroun M.; Padmashali B. Cytotoxicity and antimycobacterial properties of pyrrolo[1,2-a]quinoline derivatives: Molecular target identification and molecular docking studies. *Antibiotics*, 2020, 9, 233. <https://doi.org/10.3390/antibiotics9050233> PMID: 32392709
 20. Joshi S.D.; Devendra Kumar.; Prem Kumar S.R. Synthesis and antitubercular activity of some novel N'-substituted benzene sulphonamide derivatives. *Ind. J. Hetero. Chem.*, 2018, 28(4), 441–446.
 21. Tasdemir D.; Topaloglu B.; Perozzo R.; Brun R.; O'Neill R.; Carballeira N.M.; Zhang X.; Tonge P.J.; Linden A.; Rüedi P. Marine natural products from the Turkish sponge *Agelas oroides* that inhibit the enoyl reductase from *Plasmodium falciparum*, mycobacterium tuberculosis and *Escherichia coli*. *Biorg Med Chem.* 2007, 15, 6834–6845.

22. Oliveira J.S.; Vasconcelos I.B.; Moreira I.S.; Santos D.S.; Basso L.A. Enoyl reductases as targets for the development of anti-tubercular and anti-malarial agents. *Curr Drug Targets*. 2007, 8, 399–411. <https://doi.org/10.2174/138945007780058942> PMID: 17348833
23. Teneva Y.; Simeonova R.; Valcheva V.; Angelova V.T. Recent Advances in Anti-Tuberculosis Drug Discovery Based on Hydrazone–Hydrazone and Thiadiazole Derivatives Targeting InhA. *Pharmaceuticals* 2023, 16, 484. <https://doi.org/10.3390/ph16040484> PMID: 37111241
24. Angelova V.T.; Valcheva V.; Pencheva T.; Voynikov Y.; Vassilev N.; Mihaylova R.; Momekov G.; Shivahev B. Synthesis, Antimycobacterial Activity and Docking Study of 2-Aroyl-[1]Benzopyrano[4,3-c]Pyrazol-4(1H)-One Derivatives and Related Hydrazone-Hydrazone. *Bioorg. Med. Chem. Lett.* 2017, 27, 2996–3002, <https://doi.org/10.1016/j.bmcl.2017.05.011> PMID: 28512022
25. Joshi S.D.; More U.A.; Dixit S.R.; Balmi S.V.; Kulkarni B.G.; Ullagaddi G.; Lherbet C.; Aminabhavi T.M. Chemical synthesis and *in silico* molecular modeling of novel pyrrolyl benzohydrazide derivatives: their biological evaluation against enoyl ACP reductase (InhA) and *Mycobacterium tuberculosis*. *Bioorg. Chem.*, 2017, 75, 181–200.
26. Biava M.; Porretta G.C.; Poce G.; Battilocchio C.; Alfonso S.; de Logu A.; Manetti F.; Botta M. Developing Pyrrole-derived Antimycobacterial Agents: A Rational Lead Optimization Approach. *ChemMedChem* 2011, 6, 593–599, <https://doi.org/10.1002/cmdc.201000526> PMID: 21341373
27. Mahnashi M.H.; Koganole P.; Prem Kumar S.R.; Ashgar S.S.; Shaikh I.A.; Joshi S.D.; Alqahtani A.S. Synthesis, molecular docking study, and biological evaluation of new 4-(2,5-dimethyl-1H-pyrrol-1-yl)-N-(2-(substituted)acetyl)benzohydrazides as dual enoyl ACP reductase and DHFR enzyme inhibitors. *Antibiotics*, 2023, 12, 763. <https://doi.org/10.3390/antibiotics12040763> PMID: 37107123
28. Mahnashi M.H.; Kittur B.; Prem Kumar S. R.; Alqahtani A.S.; Ali A.A.; Alshahrani M.A.; Shaikh I.A.; Joshi S.D. *In silico* and *in vitro* evaluation of a new pyrrolyl benzohydrazide derivatives as potential antimicrobial agents. *Ind. J. Hetero. Chem.*, 2022, 32, 523–530.
29. Joshi S.D.; Vagdevi H.M.; Vaidya V.P.; Gadaginamath G.S. Synthesis of new 4-pyrrol-1-ylbenzoic acid hydrazide analogs and some derived oxadiazole, triazole and pyrrole ring systems, a novel class of potential antibacterial and antitubercular agents. *European J. Med. Chem.* 2008, 43, 1989–1996. <https://doi.org/10.1016/j.ejmech.2007.11.016> PMID: 18207286
30. Jain A.N. Surflex: Fully automatic flexible molecular docking using a molecular similarity-based search engine. *J. Med. Chem.* 2003, 46, 499–511. <https://doi.org/10.1021/jm020406h> PMID: 12570372
31. Sybyl-X Molecular Modeling Software Packages, Version 2.0; TRIPOS Associates, Inc: St. Louis, MO, USA, 2012.
32. Jain A.N. Scoring noncovalent protein-ligand interactions: A continuous differentiable function tuned to compute binding affinities. *J. Comput. Aided Mol. Des.* 1996, 10, 427–440. <https://doi.org/10.1007/BF00124474> PMID: 8951652
33. Pratama M.R.F.; Poerwono H.; Siswodiharjo S. ADMET properties of novel 5-O-benzoylpinostrobin derivatives. *J. Basic Clin. Physiol. Pharmacol.* 2019, 30, 1–30. <https://doi.org/10.1515/jbcpp-2019-0251> PMID: 31851612
34. Daina A.; Michielin O.; Zoete V. SwissADME: a free web tool to evaluate pharmacokinetics, drug-likeness and medicinal chemistry friendliness of small molecules. *Sci. Rep.* 2017, 7, 42717, <https://doi.org/10.1038/srep42717> PMID: 28256516
35. Bakchi B.; Krishna A. D.; Sreecharan E.; Ganesh V. B.; Niharika M.; Maharshi S.; Puttagunta S.B.; Sigalapalli D.K.; Bhandare R.R.; vShaik A. B. An overview on applications of swissadme web tool in the design and development of anticancer, antitubercular and antimicrobial agents: A medicinal chemist's perspective. *J. Mol. Str.*, 2022, 1259, 132712, <https://doi.org/10.1016/j.molstruc.2022.132712>
36. Daina A.; Zoete V. Application of the Swiss Drug Design Online Resources in Virtual Screening. *Int. J. Mol. Sci.* 2019, 20, 4612, <https://doi.org/10.3390/ijms20184612> PMID: 31540350
37. Lourenco M.C.S.; deSouza M.V.N.; Pinheiro A.C.; Ferreira D.M.; Goncalves B.R.; Nogueira T.C.M. Evaluation of anti-tubercular activity of nicotinic and isoniazid analogues. *Arkivoc.* 2007, 15, 181–191.
38. Goto S.K.; Jo K.T.; Kawakita T.S.; Mitsuhashi S.T.; Nishino T.N.; Ohsawa N.; Tanami H. Method of minimum inhibitory concentration (MIC) determination, *Chemotherapy.*, 1981, 29, 76–79.
39. Zawadzka K.; Felczak A.; Głowacka I.E.; Piotrowska D.G.; Lisowska K. Evaluation of the antimicrobial potential and toxicity of a newly synthesised 4-(4-(benzylamino)butoxy)-9H-carbazole. *Int. J. Mol. Sci.* 2021, 22, 12796. <https://doi.org/10.3390/ijms222312796> PMID: 34884610